

SAND REPORT

SAND2003-2897

Unlimited Release

Printed August 2003

Experimental Design and Analysis for Accelerated Degradation Tests with Li-Ion Cells

Edward V Thomas, Emanuel P. Roth, Daniel H. Doughty, and Rudolph G. Jungst

Prepared by
Sandia National Laboratories
Albuquerque, New Mexico 87185 and Livermore, California 94550

Sandia is a multiprogram laboratory operated by Sandia Corporation,
a Lockheed Martin Company, for the United States Department of
Energy under Contract DE-AC04-94AL85000.

Approved for public release; further dissemination unlimited.



Sandia National Laboratories

Issued by Sandia National Laboratories, operated for the United States Department of Energy by Sandia Corporation.

NOTICE: This report was prepared as an account of work sponsored by an agency of the United States Government. Neither the United States Government, nor any agency thereof, nor any of their employees, nor any of their contractors, subcontractors, or their employees, make any warranty, express or implied, or assume any legal liability or responsibility for the accuracy, completeness, or usefulness of any information, apparatus, product, or process disclosed, or represent that its use would not infringe privately owned rights. Reference herein to any specific commercial product, process, or service by trade name, trademark, manufacturer, or otherwise, does not necessarily constitute or imply its endorsement, recommendation, or favoring by the United States Government, any agency thereof, or any of their contractors or subcontractors. The views and opinions expressed herein do not necessarily state or reflect those of the United States Government, any agency thereof, or any of their contractors.

Printed in the United States of America. This report has been reproduced directly from the best available copy.

Available to DOE and DOE contractors from
U.S. Department of Energy
Office of Scientific and Technical Information
P.O. Box 62
Oak Ridge, TN 37831

Telephone: (865)576-8401
Facsimile: (865)576-5728
E-Mail: reports@adonis.osti.gov
Online ordering: <http://www.doe.gov/bridge>

Available to the public from
U.S. Department of Commerce
National Technical Information Service
5285 Port Royal Rd
Springfield, VA 22161

Telephone: (800)553-6847
Facsimile: (703)605-6900
E-Mail: orders@ntis.fedworld.gov
Online order: <http://www.ntis.gov/ordering.htm>



SAND2003-2897
Unlimited Release
Printed August 2003

Experimental Design and Analysis for Accelerated Degradation Tests With Li-Ion Cells

Edward V. Thomas
Independent Surveillance Assessment and Statistics Department

Emanuel P. Roth, Daniel H. Doughty, and Rudolph G. Jungst,
Lithium Battery Research and Development Department

Sandia National Laboratories
P.O. Box 5800
Albuquerque, NM 87185-0829

Abstract

This document describes a general protocol (involving both experimental and data analytic aspects) that is designed to be a *roadmap* for rapidly obtaining a *useful* assessment of the *average lifetime* (at some specified use conditions) that might be expected from cells of a particular design. The proposed *experimental protocol* involves a series of accelerated degradation experiments. Through the acquisition of degradation data over time specified by the experimental protocol, an unambiguous assessment of the effects of accelerating factors (e.g., temperature and state of charge) on various measures of the health of a cell (e.g., power fade and capacity fade) will result. In order to assess cell lifetime, it is necessary to develop a model that accurately predicts degradation over a range of the experimental factors. In general, it is difficult to specify an appropriate model form without some preliminary analysis of the data. Nevertheless, assuming that the aging phenomenon relates to a chemical reaction with simple first-order rate kinetics, a *data analysis protocol* is also provided to construct a useful model that relates performance degradation to the levels of the accelerating factors. This model can then be used to make an accurate assessment of the average cell lifetime. The proposed experimental and data analysis protocols are illustrated with a case study involving the effects of accelerated aging on the power output from Gen-2 cells. For this case study, inadequacies of the simple first-order kinetics model were observed. However, a more complex model allowing for the effects of two concurrent mechanisms provided an accurate representation of the experimental data.

Acknowledgments

This work was performed under the auspices of DOE FreedomCAR & Vehicle Technologies Office through the Advanced Technology Development (ATD) High Power Battery Development Program. Sandia is a multiprogram laboratory operated by Sandia Corporation, a Lockheed Martin Company, for the United States Department of Energy under Contract DE-AC04-94AL85000. Useful comments from Stephen V. Crowder on an earlier version of this report are acknowledged.

Contents

1.	Introduction.....	7
1.1	Organization of the Document.....	8
2.	Summary Overview of Accelerated Life Test Protocol.....	8
3.	Experimental Protocol	11
3.1	Screening Experiments	12
3.2	Primary Aging Experiments	14
3.3	Secondary Aging Experiments	15
4.	Modeling and Data Analysis.....	17
4.1	Accelerated Degradation Model	17
4.2	Analysis of Accelerated Degradation Data.....	19
4.3	Estimate of Mean Lifetime	22
4.4	Augmentation of Primary Aging Data - Design Considerations	23
4.5	Other Modeling and Data Analysis Methods.....	24
5.	Case Study – Gen2 Cells.....	24
5.1	Experimental Design (Primary Aging Experiment)	25
5.2	First Data Analysis - Following 32 weeks of Aging.....	26
5.3	Second Data Analysis - Following 44 weeks of Aging	34
6.	Summary and Future Work.....	42
7.	References.....	43
8.	APPENDIX A — Fractional Factorial Designs.....	44
9.	APPENDIX B – Plackett-Burman Design.....	47

Figures

Figure 2.1 – Flowchart for Assessing Cell Life Through Accelerated Degradation Tests.....	10
Figure 5.1 – Fit Quality versus ρ for 60% State of Charge	27
Figure 5.2 – Fit Quality versus ρ for 80% State of Charge	28
Figure 5.3 – Fit Quality versus ρ for 100% State of Charge	28
Figure 5.4 – Composite Arrhenius Plot for 60% State of Charge	29
Figure 5.5 – Composite Arrhenius Plot for 80% State of Charge	30
Figure 5.6 – Composite Arrhenius Plot for 100% State of Charge	30
Figure 5.7 – Predicted versus Observed Relative Power for 60% State of Charge	31
Figure 5.8 – Predicted versus Observed Relative Power for 80% State of Charge	32
Figure 5.9 – Predicted versus Observed Relative Power for 100% State of Charge	32
Figure 5.10 – Estimated Power Fade versus Time (with 95% confidence limits), 60% State of Charge, 25 ^o C ($\rho=1.00$)	33
Figure 5.11 – Estimated Power Fade and Observed Power Fade versus Time, 60% State of Charge, 25 ^o C ($\rho=1.00$)	34
Figure 5.12 – Relative Power versus Time (60% State of Charge)	36
Figure 5.13 – Relative Power versus Time ^{3/2} (60% State of Charge)	36
Figure 5.14 – Relative Power versus Time ^{3/2} (80% State of Charge)	37
Figure 5.15 – Relative Power versus Time ^{3/2} (100% State of Charge)	37
Figure 5.16 – Logit(<i>A</i>) versus 1/Temperature and SOC	38
Figure 5.17 – Log (<i>B</i>) versus 1/Temperature and SOC	39
Figure 5.18 – % Power Fade versus Time: 60% SOC	41
Figure 5.19 – % Power Fade versus Time: 80% SOC	41

Tables

Table 5.1 Replication at Each Experimental Condition.....	25
Table 5.2 Estimates of Model Parameters (with standard errors).....	29
Table 8.1 – 3 Factor Design.....	44
Table 8.2 – 4 Factor Design.....	44
Table 8.3 – 5 Factor Design.....	45
Table 8.4 – 6 Factor Design.....	45
Table 8.5 – 7 Factor Design.....	46
Table 9.1 – Plackett-Burman Design.....	47

Experimental Design and Analysis for Accelerated Degradation Tests With Li-Ion Cells

1. Introduction

The purpose of this document is to provide a protocol for rapidly obtaining a *useful* assessment of the *average lifetime* (at some specified use conditions) that might be expected from cells of a particular design. Emphasis is placed on understanding typical cell behavior rather than quantifying the variation in performance from cell to cell. An understanding of cell-to-cell (or battery-to-battery) variation would be critical with regard to the development of warranty policies. However, one would need to test actual production cells to effectively develop such warranty policies. Thus, the focus here is on the capability of the cell design rather than the ability to produce homogeneous cells in large quantities.

Due to the expected relatively long cell life and the need to rapidly assess cell lifetime, it is necessary to use accelerated degradation experiments as the means to estimate the average cell lifetime at normal operating conditions. Through the acquisition of appropriate degradation data over time, an unambiguous assessment of the effects of accelerating factors (e.g., temperature, charge/discharge cycles and state of charge) on various measures of the health of a cell (e.g., power fade and capacity fade) will result. Furthermore, it may be possible to construct a useful model that relates performance degradation to the levels of the accelerating factors. A good working model can be used to make an accurate assessment of the average cell lifetime.

In one important sense, the assessment of the effects of aging rechargeable cells is more straightforward than with primary cells. In the case of primary cells, it is not possible to obtain a baseline performance measurement of a cell to be aged. Hence, one is only able to relate the performance of an aged cell to some distribution of baseline performance (see e.g., Weigand and Thomas (2002)). In the case of rechargeable cells, one can relate the performance of an aged cell directly to its own baseline performance. This is extremely valuable when the variability in baseline performance is non-trivial when compared to aging effects.

It is important to have an effective and efficient experimental strategy for assessment of aging effects and developing accelerated degradation models. The experimental strategy recommended here involves a number of sequential stages. Initially, experiments might be performed to select viable accelerating factors. Follow-on experiments involving the selected factors would be used to obtain an accurate assessment of cell lifetime.

In order to make an accurate assessment of average cell lifetime it is necessary to couple the experimental protocol with effective data analysis and modeling. The emphasis here is on accurate prediction rather than mechanism identification. The development of a good working model often depends on the skill of the modeler who is analyzing the degradation data. In general, there will be at best incomplete knowledge of the specific degradation mechanisms that are involved. Thus, a modeler must often construct empirical models. Such models should be relatively simple (meaning few parameters). The approach here is to rely on the experimental data to help specify a model form. The model form needs to provide a good representation of the

experimental data. Thus, some effort must be used to establish the quality of the model form. If the degradation phenomenon is related to a chemical reaction with first-order kinetics, it is possible to prescribe a data analysis protocol that is useful for making a prediction of cell lifetime with an associated estimate of uncertainty.

1.1 Organization of the Document

The remainder of this document provides details regarding the proposed experimental and data analysis protocols. Section 2 provides a summary overview of the protocols. A flowchart is used to indicate the sequence of activities that are needed to obtain useful estimates of cell life. Section 3 contains a detailed description of the various stages of the overall experimental protocol: screening experiments, primary aging experiments, and secondary aging experiments. Section 4 describes the proposed data analysis protocol. The protocol contains procedures for estimating the parameters of an accelerated degradation model based on first-order reaction kinetics. Methods for assessing model adequacy and estimating cell lifetime are also presented. Section 5 illustrates the use of experimental and data analysis protocols with a case study involving accelerated degradation of Gen-2 cells. Section 6 discusses future research activities that might improve the experimental and data analysis protocols.

2. Summary Overview of Accelerated Life Test Protocol

The purpose of this section is to provide a summary overview of the proposed protocol as well as a roadmap for using this document. The protocol is comprised of a number of activities that are summarized in the form of a list. Each activity is briefly described and referenced to the appropriate sections in the document that have relevant details. Accompanying this list is a flowchart (Figure 2.1).

- 1. Design Screening Experiment to Identify Accelerating Factors** – The purpose of performing a screening experiment is to select one or more factors (from a candidate pool of factors) to be used as accelerating factors in the more extensive primary aging experiments that follow. This step is not needed if accelerating factors are known. See Section 3.1.1.
- 2. Perform Screening Experiment to Identify Accelerating Factors**
- 3. Analyze Results from Screening Experiment** – Select accelerating factors based on experimental data. See Section 3.1.2.
- 4. Design Primary Aging Experiment** – The objectives of primary aging experiments are to determine empirically the effects of the accelerating factors on cell performance and to provide useful empirical models of these effects over a local region of the accelerating factors. The empirical models developed from the primary aging experiments provide

the means to obtain a basic assessment of cell lifetime. Elements of the design process include selecting test levels for the accelerating factors and the number of cells to test at each experimental condition. See Sections 3.2 and 5.1.

5. Perform Primary Aging Experiment

- 6. Develop Accelerated Degradation Model** – Develop a model relating the observed degradation over time of the selected performance metric(s) to the levels of the accelerating factors. The model should be able to extrapolate accurately in time at levels of the accelerating factors that are representative of use conditions. This process is generally iterative where each iterative cycle involves model specification, model fitting, and model validation. See Sections 4, 4.1, 4.2, 5.1, 5.2, and 5.3.
- 7. Predict Cell Lifetime Using Degradation Model** – Using the degradation model, predict the point in time at which the performance of cells under some specified use conditions is degraded beyond a minimal acceptable level. See Sections 4.3, and 5.2.1.
- 8. Assess Precision of Lifetime Prediction** – See Section 5.2.1.
- 9. Design Secondary Aging Experiment** – The general objective of secondary aging experiments is to clarify results from the primary aging experiments via additional testing and analysis. For example, if the prediction of mean cell lifetime is not sufficiently precise, then it may be necessary to age (and test) additional cells in order to improve precision. Additional testing could also be used to validate accelerated degradation models developed by using the data from the primary aging experiments. See Sections 3.3, and 4.4.

10. Perform Secondary Aging Experiment

- 11. Update Degradation Model and Life Predictions With Additional Data** – Refine and/or modify degradation model. See Sections 4, 4.1, 4.2, 5.1, 5.2, and 5.3.

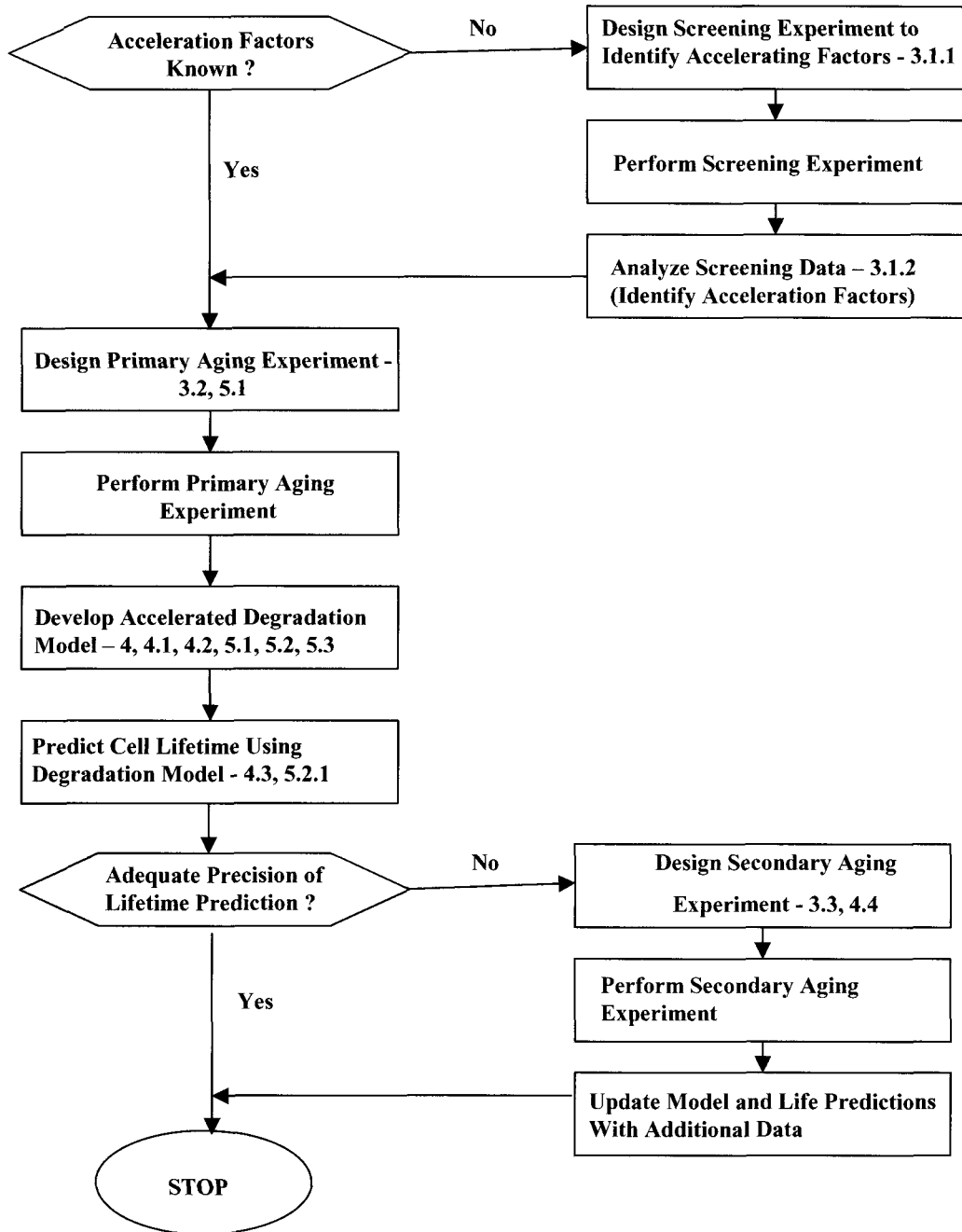


Figure 2.1 – Flowchart for Assessing Cell Life Through Accelerated Degradation Tests

3. Experimental Protocol

The overall experimental strategy could involve up to three sequential stages: screening experiments, primary aging experiments, and secondary aging experiments. The purpose of the screening experiments (which may or may not be required) is to select viable accelerating factors. One might opt to use screening experiments in cases when the cell design/chemistry is a radical departure from existing designs such that accelerating factors are unknown. The primary aging experiments represent the kernel of the experimental strategy. These experiments involve known accelerating factors and provide the means to obtain a basic assessment of cell lifetime. The secondary aging experiments (which may or may not be needed) are used to improve the basic assessment of cell lifetime as well as validate accelerated degradation models that were developed from the primary aging experiments. If necessary, the precision associated with estimates of average cell lifetime may be improved by augmenting the primary experimental design with additional testing involving more cells and/or continued aging/testing of cells associated with the primary experimental design.

Each of the three stages of the overall experimental strategy involve design and analysis issues. Many of these issues overlap across the three stages. For example, prior to proceeding with any experimentation, it is necessary to select a set of response variables that relate to the performance measures of interest (e.g., power and capacity). The set of response variables that is measured should be consistent over all stages of the experimentation.

It is also important to understand the *measurement capability* of each of the response variables that is chosen. For example, in the case of benign storage conditions, there might be only a slight degradation in a cell's performance over time. However, it is important to have the ability to resolve small changes in performance over time in order to develop accurate accelerated degradation models. Thus, it is critical that the measurement system be accurate, precise, and stable over time. Prior to beginning the aging experiments, it is necessary to have an understanding of the measurement capability associated with each of the response variables. This understanding can be acquired via a *measurement capability study* (see e.g., Speitel 1982).

Finally, it is important to understand the degree to which the measurement of cell performance affects the degradation status of the cell. Ideally, the measurement should not contribute at all to cell degradation. In practice, however, the measurement process itself will inevitably cause some degradation. In general, a more aggressive performance test will lead to more degradation. On the other hand, a more aggressive performance test may provide a more sensitive measure of the degradation status of the cell. This tradeoff between sensitivity and degradation of the measurement process should be used to influence the selection of the particular performance test to be used.

The rest of this section describes each of the three stages of the proposed experimental protocol in terms of specific objectives and design/analysis issues.

3.1 Screening Experiments

The purpose of performing a screening experiment is to select one or more factors (from a candidate pool of factors) to be used as accelerating factors in the more extensive primary aging experiments that follow (see next sub-section). The intent is to accomplish this with a minimal expenditure of resources. That is, a limited number of cells are to be aged for a relatively short period of time. One might opt to use screening experiments in cases when the cell design/chemistry is a radical departure from existing designs. Otherwise, in cases where the important acceleration factors have been identified, one does not need to conduct screening experiments.

3.1.1 Designing Screening Experiments

Designing the screening experiment involves a number of considerations. Given that suitable response variables have been selected, the first goal is to select a candidate pool of factors. A good way to accomplish this is via a brainstorming session with a group of subject-matter experts. Criteria for selecting a factor for the candidate pool include the factor's perceived ability to accelerate performance degradation as well as the experimenter's ability to control the factor. It may not be necessary to include certain factors (such as storage temperature) in the candidate pool if it is known that they will be involved in the primary aging experiments. Once the candidate pool of factors has been fixed, it is necessary to select two level settings for each factor (denoted least and most accelerating). For the *least* accelerating level, one should choose a benign use condition. For the *most* accelerating level it is important to choose a level far enough away from the benign level such that there is a reasonable chance for observing accelerated performance degradation in a relatively short period of time.

The literature contains a number of plans that specify the number and particular pattern of experimental conditions to be studied when the goal is to screen factors (e.g., see Box and Draper (1987) and Box, Hunter, and Hunter (1978)). These plans are often referred to as main effects plans. Two general families of plans are recommended here: fractional factorial designs and Plackett-Burman designs. Fractional factorial designs are recommended when there are seven or fewer factors in the candidate pool. Otherwise, in the rare instances where there are more than seven factors in the candidate pool, Plackett-Burman designs are recommended. Appendix A provides tables of fractional factorial designs for cases with three to seven candidate factors. Appendix B provides a Plackett-Burman design that can be used in cases where there are up to eleven candidate factors.

Each table provides a list of experimental conditions. Each experimental condition is defined in terms of the settings of each of the factors ('-' denotes the perceived least accelerating level, while '+' denotes most accelerating level). In the case of the Plackett-Burman design, to be used when there are from 8-11 factors in the candidate pool, an experimental condition is defined by using columns F1-F8 (8 factors), F1-F9 (9 factors), F1-F10 (10 factors), and F1-F11 (11 factors). It is recommended that at least two cells be randomly assigned to each experimental condition. The cells should be from a homogeneous production lot.

Following a sufficient time allocated for aging the cells, they should be removed from storage and tested. Separate analyses of the experimental results for each response variable are used to select accelerating factors to be used in the more extensive primary aging experiments.

3.1.2 Analysis of Screening Data

Using hypothetical results from a three-factor design with r replicates per experimental condition (see Table 2.1.1), the steps of analyzing the effect of a specific factor on an individual response variable are illustrated as follows.

Table 2.1.1 – Hypothetical Results from Three-factor Experiment

Experimental Condition	Factor#1	Factor#2	Factor#3	Average Response	Standard Deviation of Response
1	-	-	+	M_1	S_1
2	-	+	-	M_2	S_2
3	+	-	-	M_3	S_3
4	+	+	+	M_4	S_4

1. Compute a pooled estimate of cell-to-cell standard deviation (within treatment)

$$S_{pool} = \sqrt{\frac{1}{n} \cdot \sum_{i=1}^n S_i^2}, \text{ where } n \text{ is the number of experimental conditions}$$

2. Estimate the main effect of each factor. Find the average difference between the response variable when a specific factor is at high level (+) versus low level (-).

$$\text{Factor\#1: } M.E.(1) = \frac{M_3 + M_4 - (M_1 + M_2)}{2}$$

$$\text{Factor\#2: } M.E.(2) = \frac{M_2 + M_4 - (M_1 + M_3)}{2}$$

$$\text{Factor\#3: } M.E.(3) = \frac{M_1 + M_4 - (M_2 + M_3)}{2}$$

3. Compute the least significance difference (LSD) for assessing factor effects.

$$LSD = 3 \cdot \sqrt{\frac{4 \cdot S_{pool}^2}{n \cdot r}}, \text{ where } r \text{ is the number of replicates (cells) per experimental condition.}$$

4. Compare each estimated main effect with *LSD*. A main effect is statistically significant if it exceeds the *LSD*.
5. Rank the statistically significant main effects.

A list of the top ranked statistically significant factors should be developed for each response variable. If the lists are consistent across response variables, then the top ranked factors should be considered for use in the primary aging experiments. If the lists are inconsistent, some prioritization of the responses will be necessary.

3.2 Primary Aging Experiments

The objectives of primary aging experiments are to determine empirically the effects of the accelerating factors on the response variables of interest and to provide useful empirical models of these effects over a local region of the accelerating factors. The area of statistical methodology that relates to these objectives is *response surface methodology* (e.g., see Box and Draper (1987)). The empirical models developed from the primary aging experiments provide the means to obtain a basic assessment of cell lifetime.

Designing the primary aging (response surface) experiment involves a number of considerations. Accelerating factors are selected based on the results of screening experiments or basic subject-matter knowledge. The levels of the accelerating factors also need to be selected. In general, it is recommended that 3 levels be selected for each accelerating factor. The levels should be uniformly spaced over an interval that is sufficiently wide to observe differences in effects between levels while not so wide such that the response is highly nonlinear across the levels of a factor. It is also assumed that the degradation mechanism is consistent across the range of factor levels and the use conditions of the cell. The *least accelerating level* of each factor should be chosen to be close to the target-use condition of the cell. The *most accelerating level* of each factor should be chosen to provide the maximum acceleration without changing the mechanism for degradation. In there is some question regarding where the mechanism change occurs, one might select four levels where the fourth level is used to explore in the vicinity of where the mechanism is perceived to change.

Once the accelerating factors and associated factor levels have been determined it is necessary to specify the set of experimental conditions to be examined. With fewer than 4 accelerating factors, full factorial designs are recommended. Full factorial designs involve every possible combination of factor levels. For example, suppose that there are 2 factors each involving 3 levels. Then there are 3^2 or 9 possible experimental conditions. In unusual cases where there are 4 or more factors, other more complex designs are recommended. Chapter 15 in Box and Draper (1987) provides a number of possible designs with a minimal number of experimental conditions to consider when the number of factors exceeds four.

Once the experimental conditions have been specified, cells need to be allocated to each experimental condition. It is recommended that at least two (and preferably three) cells be allocated to each experimental condition. If available, 5-10 additional cells should be allocated

to the least-accelerating conditions (perhaps representing use conditions) in order to help resolve small changes in performance over time. Such cells could be kept on test indefinitely to serve to validate predictions of cell life. Another important design issue is to select the times at which cells are removed from storage and tested. In order to minimize resource expenditures associated with testing, we recommend testing at intervals that are uniformly spaced in log time. For example, in the case of a 64-week study, we would recommend measuring cell performance at the following time points:

{0 weeks (initial pre-aging), 2 weeks, 4 weeks, 8 weeks, 16 weeks, 32 weeks, 64 weeks}.

However, some flexibility to adapt the schedule should be maintained. For example, if after 8 weeks it is determined that cells are aging more rapidly than expected one would want to measure cells more frequently. Conversely, a reason to measure/test cells relatively infrequently is that the testing (itself) may degrade cells (see Section 5.3).

All cells should be measured prior to aging (0 weeks). However, it is not necessary to measure all of the cells at all of the other time points. For example, in the case of cells that are exposed to benign aging conditions it may not be particularly informative to acquire measurements early in the experiment since the degree of degradation may not even be detectable. Also, once a cell has degraded substantially beyond a certain performance level that reflects its useful life (see Section 3.3), its continued degradation may be affected by unrelated degradation mechanisms. Hence, such additional data may not be useful for assessing cell lifetime.

3.3 Secondary Aging Experiments

The general objective of secondary aging experiments is to clarify results from the primary aging experiments via additional testing and analysis. For example, if the uncertainty limits associated with mean cell lifetime are not sufficiently precise, then it may be necessary to age (and test) additional cells in order to improve precision (see Section 4.4). Additional testing could also be used to validate accelerated degradation models developed by using the data from the primary aging experiments. Furthermore, one could use additional testing to assess whether performance degradation of a cell beyond its current performance state depends only on its current state and not how it reached that state (see Section 4.3).

3.3.1 Improved Precision of Cell Life Estimate

If the objective is to improve precision of the estimate of cell life, then it may be necessary to augment the primary aging data with data from additional cells to be aged. Section 4.4 gives a method for assessing the expected effect of aging/testing additional cells (under some specified aging conditions) on the uncertainty interval associated with mean cell lifetime. First, however, one needs to evaluate the current uncertainty of lifetime estimates and establish the needed level of uncertainty.

Once the required level of uncertainty is established, the design issues relate to selecting experimental conditions at which to accelerate the aging of the additional cells. In general, the number of experimental conditions associated with the additional cells should be minimized.

The current model form should be used to guide the selection of levels associated with the accelerating factors. It is recommended that the secondary aging experiments follow a 2^k full factorial design where there are k accelerating factors that are deemed to be important. The *low level* of acceleration used for each factor should correspond to the lowest level used in the primary aging experiment. The *high level* of acceleration used for each factor should correspond to the highest level used in the primary aging experiment that is consistent with the developed model, associated data, and perceived mechanism. In some cases, an intermediate acceleration level for a factor could be considered when a quadratic term is used for that factor in the developed model.

Once the experimental conditions have been selected it is necessary to specify the testing scenario given by the number of cells to test at each experimental condition as well as their respective storage times/measurement intervals. Assuming that cell degradation approximately follows first-order rate kinetics with a single mechanism in a single aging environment, the method described in Section 4.4 can be used as a tool to evaluate various testing scenarios. Various scenarios can be compared with the tool. Once a satisfactory scenario has been found that will satisfy the precision requirement, it is selected for use in the actual experiment.

3.3.2 Other Objectives

1. Continue surveillance of cells under benign aging conditions to validate model.
2. Start new cells under benign aging conditions to validate model.
3. Modify storage conditions of current cells and monitor performance to assess whether performance degradation of a cell beyond its current performance state depends only on its current state and not how it reached that state (see Section 3.3).
4. Some cells might be kept in reserve for validating the various aging models (or resolving inconsistencies) that result from the primary aging experiment. Such cells could be put on test any time after the initiation of the primary aging experiment.

4. Modeling and Data Analysis

In general, a model relating the observed degradation of the response variables to the accelerating factors is needed in order to estimate the average cell lifetime. In order to provide a valid estimate of cell lifetime, the model should be able to extrapolate accurately in time at levels of the accelerating factors that are representative of use conditions. In general, a trained analyst who is familiar with the subject matter best performs the modeling process. This process is generally iterative where each iterative cycle involves model specification, model fitting, and model validation. The process is complete when the analyst is satisfied that the current model is sufficiently accurate for the conditions for which it is to be used.

The general analysis process can be summarized as follows.

1. Conduct pre-modeling exploratory analysis to identify structure and anomalies in data.
2. Develop simplest model that adequately fits experimental data over the widest range of experimental conditions.
3. Estimate model parameters with data restricted to experimental region that produces a *consistent* response to experimental conditions.
4. Validate model and check for model inaccuracy with various diagnostics.
5. Use fitted model to estimate mean cell lifetime (with estimates of uncertainty).

It is important to emphasize that the validity of the results derived from the modeling process depends on assumptions that might be difficult to verify. While small deviations from the assumptions could have minor effects on the validity of results, large deviations could have a major impact. We are not concerned about small deviations from the assumptions as our ultimate goal is to have a useful working approximation of cell behavior.

4.1 Accelerated Degradation Model

In this document, it is not possible to enumerate all possibilities regarding accelerated degradation models. Rather, we choose to focus on a single model formulation that is general enough that it could be useful in a number of battery applications. Following Castellan (1971), we assume a chemical reaction, $A \rightarrow \text{Reaction Products}$, where the reaction is first-order with respect to A . Thus, the rate law is $\frac{-d[A]}{dt} = k \cdot [A]$, where $[A]$ is the concentration of A , k is the

rate constant, and t is time. If $\log(k) = \beta_0 + \beta_1 \cdot \frac{1}{T}$, where T is the absolute temperature and β_0 and β_1 are parameters, then the Arrhenius model follows. That is,

$$[A(t)] = [A(0)] \cdot \exp\left\{-\exp\left(\beta_0 + \beta_1 \cdot \frac{1}{T}\right) \cdot t\right\}. \quad (1)$$

β_0 is often referred to as the *pre-exponential factor* while the activation energy (E_A) is given in terms of β_1 (i.e., $E_A = -R \cdot \beta_1$).

In accelerated degradation experiments we might observe some measure of performance (such as capacity or power) over various storage temperatures and time. Let $P(X;t)$ denote a generic performance metric at $X = T^{-1}$ and time, t . Following the Arrhenius model, we have

$$P(X;t) = P(X;0) \cdot \exp\{-\exp(\beta_0 + \beta_1 \cdot X) \cdot t\}. \quad (2)$$

There are a number of ways that this basic equation could be generalized with respect to the effects of time and additional accelerating factors. If we assume that there are “ q ” accelerating factors (X_1, X_2, \dots, X_q), we might consider models of the form

$$P(X_1, X_2, \dots, X_q; t) = P(X_1, X_2, \dots, X_q; 0) \cdot \exp\{-\exp(f(X_1, X_2, \dots, X_q)) \cdot t^\rho\}, \quad (3)$$

where, for example, $f(X_1, X_2, \dots, X_q) = \beta_0 + \sum_{j=1}^q \beta_j \cdot X_j + \sum_{j \neq k} \beta_{jk} \cdot X_j \cdot X_k + \sum_{j=1}^q \beta_{jj} \cdot X_j^2$.

Here, $f(\cdot)$ is a *quadratic response surface* that can provide a useful approximation to any smooth function of the arguments of $f(\cdot)$ over some local region of interest. This approach is very common and useful when developing empirical models from experimental data (see e.g., Box and Draper (1987)).

The general form of the model can be re-expressed as

$$Z(X_1, X_2, \dots, X_q; t) = \frac{P(X_1, X_2, \dots, X_q; t)}{P(X_1, X_2, \dots, X_q; 0)} = \exp\{-\exp(f(X_1, X_2, \dots, X_q)) \cdot t^\rho\}, \quad (4)$$

where $Z(\cdot)$ is the value of the performance metric relative to its value at $t = 0$. By assuming that $0 \leq P(X_1, X_2, \dots, X_q; t) \leq P(X_1, X_2, \dots, X_q; 0)$, $0 \leq Z(X_1, X_2, \dots, X_q; t) \leq 1$. Further, note that $Z(X_1, X_2, \dots, X_q; t = 0) = 1$ and $Z(X_1, X_2, \dots, X_q; t = \infty) = 0$.

Further re-expression of equation (4) leads to

$$\log\left\{\frac{-\log(Z(X_1, X_2, \dots, X_q; t))}{t^\rho}\right\} = f(X_1, X_2, \dots, X_q). \quad (5)$$

Re-expressing equation (2) in this way leads to

$$\log\left\{\frac{-\log(Z(X;t))}{t}\right\} = \beta_0 + \beta_1 \cdot X, \text{ where } X = T^{-1}. \quad (6)$$

Re-expressing equation (3) leads to

$$\log\left\{\frac{-\log(Z(X_1, X_2, \dots, X_q; t))}{t^\rho}\right\} = \beta_0 + \sum_{j=1}^q \beta_j \cdot X_j + \sum_{j < k} \beta_{jk} \cdot X_j \cdot X_k + \sum_{j=1}^q \beta_{jj} \cdot X_j^2. \quad (7)$$

For a fixed value of ρ , the above re-expressions lead to models that are linear in the remaining parameters (β s). This is useful as linear regression with its associated theory and methods is applicable and can be used to make inference concerning the β s.

4.2 Analysis of Accelerated Degradation Data

The general model described in equation (7) of the previous section is used as a template for developing a specific model that represents the experimental data associated with a particular cell design. In order to develop a useful specific model, a number of issues need to be addressed. Foremost among these issues is the need to identify which of the potential predictor variables $\{X_j, X_j \cdot X_k, X_j^2\}_{j=1 \dots q, j < k}$ contributes significantly to explaining variation in cell performance.

Other issues include the estimation of ρ and the β s as well as defining the range of applicability of the model.

The *joint estimation* of ρ and the β s is complicated, since the model is not linear in ρ . However, a simple two-step process can be used to resolve this complication. First, it is assumed that a valid metric for “fit quality” exists across values of ρ . For a fixed value of ρ , the β s can be estimated directly by linear regression. For each case of ρ (and the implied estimates of the β s), the “fit quality” can be obtained. Thus, one can compare model fits across values of ρ and select a value for ρ based on that metric. With ρ selected, the estimated β s are determined by linear regression.

One natural metric for “fit quality” is $\sum_{i=1}^n (\hat{Z}_i - Z_i)^2$, where Z_i is the observed value of the normalized performance metric for the i^{th} observation, and \hat{Z}_i is the predicted value of the normalized performance metric for the i^{th} observation. For example, in the case of equation (6),

$$\hat{Z}_i = \exp\left\{-\exp\left(\hat{\beta}_0 + \hat{\beta}_1 \cdot \frac{1}{T_i}\right) \cdot t_i^{\hat{\rho}}\right\},$$

where $\hat{\beta}_0$, $\hat{\beta}_1$, and $\hat{\rho}$ are the parameter estimates, and T_i and t_i are the storage temperature and aging time associated with the i^{th} observation.

4.2.1 Accelerated Degradation Data

At designated points in time (t), cell performance is measured. The experimental data consist of these performance data. It is assumed that the levels of the accelerating factors (X_1, X_2, \dots, X_q) are constant for a given cell, but vary from cell to cell. Let the initial measurement of the c^{th} cell be denoted by $P_c(X_1, X_2, \dots, X_q; 0)$. Subsequent measurements of the c^{th} cell at $t_1, t_2, \dots, t_{n(c)}$ are

denoted by $P_c(X_1, X_2, \dots, X_q; t_1), P_c(X_1, X_2, \dots, X_q; t_2), \dots, P_c(X_1, X_2, \dots, X_q; t_{n(c)})$. The performance of the cell at time t relative to when it was measured prior to aging is

$Z_c(X_1, X_2, \dots, X_q; t) = \frac{P_c(X_1, X_2, \dots, X_q; t)}{P_c(X_1, X_2, \dots, X_q; 0)}$. Thus, there are $n(c)$ observations associated with the c^{th} cell: $Z_c(X_1, X_2, \dots, X_q; t_1), Z_c(X_1, X_2, \dots, X_q; t_2), \dots, Z_c(X_1, X_2, \dots, X_q; t_{n(c)})$.

Assuming that better performance corresponds with a larger value for the performance measure P , one would expect that

$$1 > Z_c(X_1, X_2, \dots, X_q; t_1) > Z_c(X_1, X_2, \dots, X_q; t_2), \dots, > Z_c(X_1, X_2, \dots, X_q; t_{n(c)}).$$

For the analysis that follows, it is imperative that $Z_c(X_1, X_2, \dots, X_q; t) < 1$ for all values of t that exceed 0. Observations where $Z_c(X_1, X_2, \dots, X_q; t) \geq 0$ are *excluded* from analysis. If no observations are excluded there are $N = n(1) + n(2) + \dots + n(C)$ observations from C cells. So for the i^{th} observation, the summary information consists of the cell (c_i), the aging time (t_i), the levels of the accelerating factors ($X_{i1}, X_{i2}, \dots, X_{iq}$), and the

response $Y_i = \log \left\{ \frac{-\log(Z(X_{i1}, X_{i2}, \dots, X_{iq}); t_i)}{t_i^\rho} \right\}$.

4.2.2 Generalized Least-Squares Regression

The computational aspects of linear regression are well known and can be found, for example, in Draper and Smith (1981). Here, a generalization of linear regression (generalized least-squares regression, e.g., see Ripley 1981) is used to estimate the model parameters. This generalization is needed to accommodate the particular error structure that is present in the re-expressed aging data.

To continue, refer to equation (7) and assume a value for ρ has been selected. Then

$$Y(X_1, X_2, \dots, X_q) = \log \left\{ \frac{-\log(Z(X_1, X_2, \dots, X_q; t))}{t^\rho} \right\} \text{ factors out the effect of } t \text{ resulting in}$$

$$Y(X_1, X_2, \dots, X_q) = \beta_0 + \sum_{j=1}^q \beta_j \cdot X_j + \sum_{j \neq k} \beta_{jk} \cdot X_j \cdot X_k + \sum_{j=1}^q \beta_{jj} \cdot X_j^2.$$

To put this context of the experimental data set some additional notation is required. Let X_{ij} be the level of the j^{th} experimental factor for the i^{th} observation and let Y_i be the associated response. Then,

$$Y_i = \beta_0 + \sum_{j=1}^q \beta_j \cdot X_{ij} + \sum_{j \neq k} \beta_{jk} \cdot X_{ij} \cdot X_{ik} + \sum_{j=1}^q \beta_{jj} \cdot X_{ij}^2 + \varepsilon_i, \quad (8)$$

where ε_i is a random error term that is added to represent variation due to cell-to-cell effects and measurement error associated with the i^{th} of N observations. Note that equation (8) represents the full quadratic model in the accelerating factors. In most cases, relatively few of the model terms will be used (e.g., see Section 5). Empirically, we have found that the variance of ε_i

depends on Z_i via $Var(\varepsilon_i) = \sigma_i^2 \propto \frac{1}{\log(Z_i)}$. The relative importance of cell-to-cell effects will

likely vary from experiment to experiment. That can be modeled by considering the covariance between ε_i and ε_h ($Cov(\varepsilon_i, \varepsilon_h)$), where $i \neq h$. The form for $Cov(\varepsilon_i, \varepsilon_h)$ depends on whether or not the i^{th} and h^{th} observations are from the same cell. If the i^{th} and h^{th} observations are not from the same cell, then $Cov(\varepsilon_i, \varepsilon_h) = 0$. If the i^{th} and h^{th} observations are from the same cell, then $Cov(\varepsilon_i, \varepsilon_h) = \lambda \cdot \sigma_i \cdot \sigma_h$, where $0 \leq \lambda \leq 1$. Let Ω consist of the $N \times N$ matrix with diagonal

elements $\frac{1}{\log(Z_i)}$ and off-diagonal elements $\Omega_{ih} = \lambda \cdot \sqrt{\frac{1}{\log(Z_i)} \cdot \frac{1}{\log(Z_h)}}$ when the i^{th} and h^{th}

observations are from the same cell and zero otherwise. The generalized least-squares estimate of the model parameters is given by the $(p+1) \times 1$ vector $\hat{\beta} = (X_a^T \cdot \Omega^{-1} \cdot X_a)^{-1} \cdot X_a^T \cdot \Omega^{-1} \cdot Y$, (9)

where X_a is a $N \times (p+1)$ augmented matrix of explanatory variables and Y is a $N \times 1$ vector of responses. The first column of X_a is a vector of ones. Each of the other p columns of X_a correspond to other model terms. Possible model terms include any of the q linear terms

(X_j) , $\frac{q \cdot (q-1)}{2}$ interactive terms $(X_j \cdot X_k)$, and q quadratic terms (X_j^2) in equation (8). Thus,

$p \leq 2 \cdot q + \frac{q \cdot (q-1)}{2}$. Note that in many cases p will be much smaller than that upper limit as

only a few of the model terms will be used. For example, if the X_1 term is included in the model, then one column of X_a is $(X_{11}, X_{21}, \dots, X_{N1})^T$.

It is advisable to iterate the estimation process once, where Ω is reconstructed with

$Var(\varepsilon_i) = \sigma_i^2 \propto \frac{1}{\log(\hat{Z}_i)}$, where $\hat{Z}_i = \exp\{-\exp(\mathbf{x}_i \cdot \hat{\beta}_{init}) \cdot t_i^{\hat{\rho}}\}$, \mathbf{x}_i is the i th row of X_a and $\hat{\beta}_{init}$ is the

initial estimate of β . The final estimate of β , based on (9) with the reconstructed Ω is $\hat{\beta}_{final}$.

Assuming that Ω is proportional to the unknown error covariance matrix, the covariance of

$\hat{\beta}_{final}$ is estimated to be $Cov(\hat{\beta}_{final}) = (X_a^T \cdot \Omega^{-1} \cdot X_a)^{-1} \cdot \hat{\sigma}_{res}^2$, where

$$\hat{\sigma}_{res}^2 = \frac{1}{(n - (p+1))} \sum_{i=1}^N \left(\Omega^{-1/2} \cdot \mathbf{x}_i \cdot \hat{\beta}_{final} - \Omega^{-1/2} \cdot Y_i \right)^2.$$

Note that in order to produce stable estimates of the model parameters it may be useful to center all columns (except the first) of X_a . This is particularly true if quadratic terms are used in the model (see, e.g. Draper and Smith (1981) pp. 488-489).

4.2.2.1 Analysis of Cell-to-Cell Effects

In order to produce valid estimates of the uncertainty in the model parameters, Ω must be constructed with a value for λ that is supported by the experimental data. A simple procedure to find a representative value for λ is as follows.

1. Compute normalized prediction errors over all observations:
$$NPE_i = \frac{\mathbf{x}_i \cdot \hat{\boldsymbol{\beta}} - Y_i}{\sqrt{\frac{1}{\log(\hat{Z}_i)}}}$$

2. Compute the standard deviation of the NPE_i : $\sigma_{NPE(overall)}$

3. Compute the standard deviation of the NPE within each cell: $\sigma_{NPE(c)} : c = 1 : numcells$

4. Compute overall within-cell standard deviation of NPE:

$$\sigma_{NPE-withincell} = \sqrt{\frac{(n_1 - 1) \cdot \sigma_{NPE(1)}^2 + (n_2 - 1) \cdot \sigma_{NPE(2)}^2 + \dots + (n_{numcells} - 1) \cdot \sigma_{NPE(numcells)}^2}{(n_1 - 1) + (n_2 - 1) + \dots + (n_{numcells} - 1)}}$$

5. Estimate λ :
$$\hat{\lambda} = \frac{\sigma_{NPE(overall)}^2 - \sigma_{NPE-within}^2}{\sigma_{NPE(overall)}^2}$$

4.3 Estimate of Mean Lifetime

It is assumed that the lifetime of a cell (denoted by t_{life}) is the point in time at which its relative performance has degraded to a certain minimal acceptable level. Meeker, Escobar, and Lu (1998) refer to this situation as a *soft failure*. This threshold level of performance will likely be application dependent. Here, for discussion, we assume that the threshold is defined in terms of Z from equation (4) as Z_{thresh} . Then, for a static set of conditions associated with the

accelerating factors defined by $\mathbf{x}_s = (X_1, X_2, \dots, X_q)^T$,
$$\log\left\{\frac{-\log(Z_{thresh}(X_1, X_2, \dots, X_q))}{t_{life}^\rho}\right\} = \mathbf{x}_{s-a} \boldsymbol{\beta},$$

where \mathbf{x}_{s-a} is the $(p+1)$ -dimensional vector of model terms derived from \mathbf{x}_s . An estimate of the *mean cell lifetime* at the specified set of aging conditions is given by

$$\hat{t}_{life} = \exp\left\{\frac{\log(-\log(Z_{thresh})) - \mathbf{x}_{s-a} \hat{\boldsymbol{\beta}}_{final}}{\rho}\right\}. \text{ Taking } \rho \text{ to be fixed, a measure of the uncertainty of}$$

the estimated lifetime is its approximate variance given by $Var(\hat{t}_{life}) = \hat{t}_{life}^2 \cdot \mathbf{x}_{s-a}^T \cdot Cov(\hat{\boldsymbol{\beta}}_{final}) \cdot \mathbf{x}_{s-a}$.

If the estimation errors in $\hat{\boldsymbol{\beta}}_{final}$ are assumed to be normal, then an approximate 95% confidence interval for the mean cell lifetime is $\hat{t}_{life} \pm 2 \cdot \sqrt{Var(\hat{t}_{life})}$.

The current experimental design and data analysis protocols can provide lifetime assessments that relate to the degradation of cells that age in a *constant environment*. In its actual use, a cell

may experience a wide range of environments. Thus, it is of interest to characterize cell degradation in a dynamic environment. For example, consider aging in a dynamic environment where $T(\tau)$ and $SOC(\tau)$ are the aging temperature and state of charge at time τ . Let's assume that the performance degradation of a cell beyond its current performance state depends only on its current state and not how it reached that state (*memoryless degradation*). Also, let $\hat{R}(\tau; T(\tau), SOC(\tau), \Theta)$ be the estimated rate of degradation (of relative power) at time τ , where Θ are the model parameters relating the rate of degradation to temperature and SOC. Following Chan and Meeker (2001), the cumulative degradation at time t is predicted by the model to be

$\hat{D}(t; T[0, t], SOC[0, t], \Theta) = \int_0^t \hat{R}(\tau; T(\tau), SOC(\tau), \Theta) d\tau$, where $T[0, t]$ and $SOC[0, t]$ represent the paths of temperature and SOC over the time interval $[0, t]$. Therefore, the predicted relative power is $\hat{Z}(t; T[0, t], SOC[0, t], \Theta) = 1 - \hat{D}(t; T[0, t], SOC[0, t], \Theta)$. In the case of the model

developed using data from static aging conditions, $\hat{R}(\tau; T(\tau), SOC(\tau)) = \frac{d}{d\tau} \hat{Z}(\tau; T, SOC)$. To assess whether the model developed for static aging is valid for dynamic environments, one would compare the power degradation that is observed experimentally over a variety of dynamic aging environments with the model predictions based on those same aging environments:

$\hat{D}(t; T[0, t], SOC[0, t], \Theta)$. Currently, methods for selecting the dynamic aging environments to be used for developing and/or validating degradation models are unavailable and thus could be the subject for some valuable research.

4.4 Augmentation of Primary Aging Data - Design Considerations

If the uncertainty of mean cell lifetime is larger than desired, then it may be necessary to augment the primary aging data with data from additional cells to be aged (see Section 3.3). In this section we present a method for assessing the expected effect of aging/testing additional cells (under some specified aging conditions) on the uncertainty interval associated with mean cell lifetime. For this discussion some additional notation is needed.

Let $X_{primary}$ be the $N \times (p+1)$ matrix of exploratory variables associated with the primary experiment. Each column of $X_{primary}$ captures the N values of each model term. Let $X_{secondary}$ be the $M \times (p+1)$ matrix of exploratory variables associated with a proposed secondary experiment.

In the case of the primary experiment, $Var(\hat{t}_{life}) = \hat{t}_{life}^2 \cdot \mathbf{x}_{s-a}^T \cdot Cov(\hat{\beta}_{final}) \cdot \mathbf{x}_{s-a}$, where

$Cov(\hat{\beta}_{final}) = (X_{primary}^T \cdot \Omega_{primary}^{-1} \cdot X_{primary})^{-1} \cdot \hat{\sigma}_{res}^2$, and

$$\hat{\sigma}_{res}^2 = \frac{1}{(n - (p+1))} \sum_{i=1}^N \left(\Omega_{primary}^{-1/2} \cdot X_{primary(i)} \cdot \hat{\beta}_{final} - \Omega_{primary}^{-1/2} \cdot Y_i \right)^2.$$

The expected outcome of augmenting data from the primary experiment with data from the proposed secondary experiment is to reduce the uncertainty in the model parameters and hence by association uncertainty in the mean cell lifetime. Let X_{all} be the $(N+M) \times (p+1)$ matrix of exploratory variables associated with the primary and proposed secondary experiments. Let

$\hat{Z}_{all(i)} = \exp\left\{-\exp\left(\mathbf{X}_{all(i)} \cdot \hat{\boldsymbol{\beta}}_{final}\right) \cdot t_{all(i)}^{\hat{\rho}}\right\}$. For cells to be tested in the proposed secondary experiment $t_{all(i)}$ represents the proposed level of aging. Construct $\boldsymbol{\Omega}_{all}$ as

a $(N + M) \times (N + M)$ matrix with diagonal elements $\frac{1}{\log(\hat{Z}_{all(i)})}$ and off-diagonal elements

$\Omega_{ih} = \lambda \cdot \sqrt{\frac{1}{\log(\hat{Z}_{all(i)})} \cdot \frac{1}{\log(\hat{Z}_{all(h)})}}$ when the i^{th} and h^{th} observations are from the same cell and zero otherwise. Then,

$Var(\hat{t}_{life}) = \hat{t}_{life}^2 \cdot \mathbf{x}_{s-a}^T \cdot \left((\mathbf{X}_{all}^T \cdot \boldsymbol{\Omega}_{all}^{-1} \cdot \mathbf{X}_{all})^{-1} \cdot \hat{\sigma}_{res}^2 \right) \cdot \mathbf{x}_{s-a}$. One can evaluate $Var(\hat{t}_{life})$ to assess whether or not the precision requirement is met.

4.5 Other Modeling and Data Analysis Methods

The modeling approach that is discussed here involves transforming the degradation data to be compatible with a linear model in the accelerating factors. The advantage of this approach is that it allows for the use of standard statistical linear models theory and methods for estimation and inference. There are a number of other approaches for modeling degradation data that are described in the literature. See, for example, Meeker and Escobar (1998), Meeker, Escobar, and Lu (1998), and Boulanger and Escobar (1994). Often, *maximum likelihood* methods are used to estimate model parameters when a linear model is not plausible (see e.g., Meeker, Escobar, and Lu (1998)). *Bootstrap* resampling methods can be used to develop confidence limits for model parameters and lifetime predictions in cases when the modeling process is complex (see Efron and Tibshirani (1993)).

5. Case Study – Gen2 Cells

In conjunction with the Partnership for a New Generation of Vehicles (PNGV), the Advanced Technology Development (ATD) Program was initiated in 1998 by the U.S. Department of Energy Office of Advanced Automotive Technologies to find solutions to the barriers that limit the commercialization of high-power lithium-ion batteries for hybrid electric vehicle (HEV) applications. In 2003, this program was superseded by the FreedomCAR (Freedom Cooperative Automotive Research) program that seeks to develop fuel cell based hybrid-electric vehicles. As part of this effort, the ATD Program is supporting the PNGV in the development of lithium-ion batteries for hybrid electric vehicles (HEVs). A major goal of this work is to determine the mechanism(s) of power fade and develop methods for predicting the life of lithium-ion batteries in the HEV environment. The ATD Program has been evaluating the performance of lithium-ion cells in support of this goal. Experiments were performed to investigate the effects of accelerating factors on the performance of 18650-size cells.

Here, we discuss the primary aging experiment only. A screening experiment of the type described in Section 3.1 was not performed (temperature and state of charge were identified as the accelerating factors). [The effects of cycling on cell performance degradation was not

included in this test due to insufficient number of cells.] Based on the results of the primary aging experiment, it was concluded that a secondary aging experiment was unnecessary.

Two analyses are described here (the first in Section 5.2 and the second in Section 5.3). The first analysis (based on aging data that were acquired within the first 32 weeks of the study) uses the model framework and methods that were described in Section 3.2 and is based on aging data that were acquired within the first 32 weeks. The second analysis seeks to correct inadequacies apparent in the first analysis as well as incorporate additional aging data (acquired through 44 weeks). The second analysis involves a model that allows for two concurrent degradation mechanisms.

5.1 Experimental Design (Primary Aging Experiment)

The primary aging experiment involved two accelerating factors (storage temperature and state of charge). The experiment involved four levels for storage temperature and three levels for state of charge. Four levels of storage temperature were selected, as it was not clear (before the experiment was performed) at what point the degradation mechanism changes. A full factorial design involving all possible twelve experimental conditions was selected. The amount of replication varied from 3-5 cells per experimental conditions (see Table 5.1). Use conditions are well represented by the 25°C @ 60% state of charge condition. Here, more replication was introduced at the most highly accelerated conditions. Note that in future experiments we would opt to have more replication at the least highly accelerated conditions.

Table 5.1 Replication at Each Experimental Condition

	25 degrees C	35 degrees C	45 degrees C	55 degrees C
60% State of Charge	3	3	3	3
80% State of Charge	3	3	3	5
100% State of Charge	3	3	5	5

5.1.1 Testing Details

Prior to being placed in the isothermal temperature chambers, baseline performance tests were conducted on each cell. These reference performance tests (RPTs) were used to quantify the capacity, resistance, and power of each cell (PNGV Battery Test Manual, 2001). During aging, the cells were clamped at an open-circuit voltage corresponding to 60%, 80%, or 100% SOC and underwent a once-per-day pulse profile. These RPTs were repeated every four weeks and the experiment continued up to 44 weeks. Measurement of cells that had experienced 50% or more power degradation (e.g., 55°C @ 100% state of charge) was discontinued prior to 44 weeks.

The Low Current Hybrid Pulse Power Characterization (L-HPPC) test consists of a constant-current discharge and regeneration pulse (to simulate capture of energy by “regenerative braking” of automobile) with a 32-s rest period in between, for a total duration of 60-s. The 18-s constant-current discharge pulse is performed at a 5A rate. The 10-s regeneration pulse is performed at 75% of the discharge rate (i.e., 3.75 A). This profile is repeated at every 10% depth-of-discharge (DOD) increment, with a 1-hour rest at OCV at each DOD increment to ensure that the cells have electrochemically and thermally equilibrated. All of the L-HPPC testing was performed at 25°C regardless of the aging temperature. The power fade metric used was derived from the HPPC test results and projects the power capability at the 300 Wh available energy value.

The PNGV minimum power goal for HEV batteries is 25 kW at 300 Wh available energy. This equates to about a 23% cell power fade when the appropriate power margins and scaling are applied. Thus, a cell’s lifetime is defined to be the point at which 77% of the cell’s original power remains.

5.2 First Data Analysis - Following 32 weeks of Aging

The analysis of the experimental data generally follows the discussion in Section 4.2. Here two model forms were considered. First, a *global model* that depends on the two accelerating factors: storage temperature and state of charge was considered. That is,

$$Y(X_1, X_2) = \beta_0 + \beta_1 \cdot X_1 + \beta_2 \cdot X_2, \text{ where}$$

$X_1 = T^{-1}$ (T is the storage temperature in degrees Kelvin), X_2 is the state of charge (SOC), and

$$\text{and } Y(X_1, X_2) = \log \left\{ \frac{-\log(Z(X_1, X_2))}{t^\rho} \right\}. \text{ It was determined that the global model inadequately}$$

represented the experimental data. Thus, local models (specific to each state of charge) were developed. These models are of the form

$Y(X) = \beta_0 + \beta_1 \cdot X$, where $X = T^{-1}$. Following the procedure outlined in Section 4.2, the effect of varying ρ on the quality of the model fit was investigated. Here we don’t iterate the estimation process and we assume that $\lambda = 0$ (see Section 4.2.2). Figures 5.1, 5.2, and 5.3 show how the overall model fit varies as a function of ρ . The *fit quality* was examined at 101 uniformly spaced values of ρ from .5 to 1.5. The ‘optimal’ values for ρ were found to be 1.08, 1.00, and .88 for the 60%, 80%, and 100% SOC cases, respectively. From a statistical perspective none of these values are significantly different than that obtained with $\rho = 1$. Thus, for simplicity, the additional analyses described here use $\rho = 1$ and the model

$$Y(X) = \log \left\{ \frac{-\log(Z(X))}{t} \right\} = \beta_0 + \beta_1 \cdot X.$$

Using the method described in Section 4.2.2.1 there was very little correlation detected among prediction errors from same cell. Thus, we disregard the minor correlation by setting $\lambda = 0$ in Ω .

Table 5.2 presents the parameter estimates and associated standard errors of the parameter estimates in parenthesis for each of the three cases: 60%, 80%, and 100% SOC.

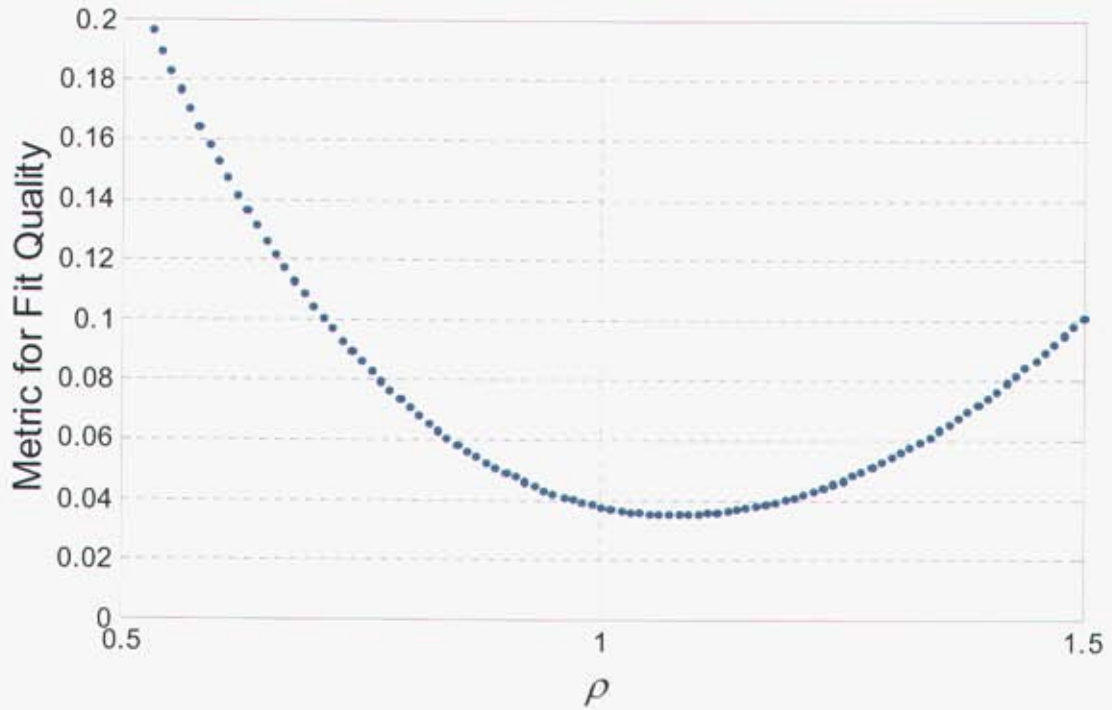


Figure 5.1 – Fit Quality versus ρ for 60% State of Charge

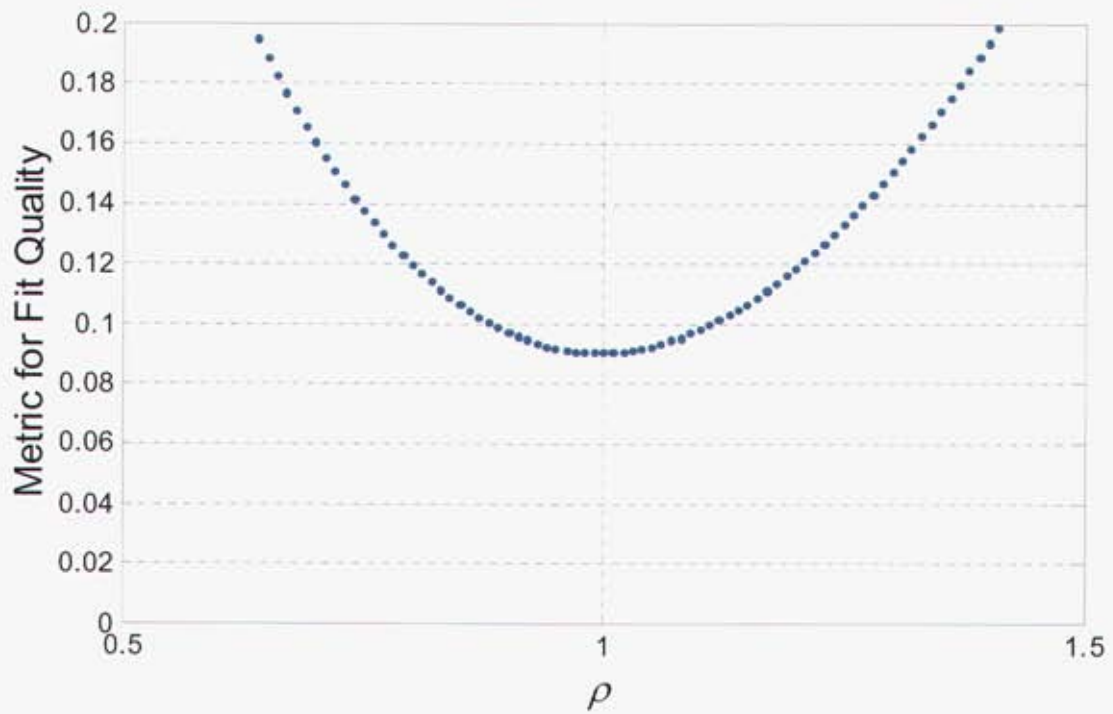


Figure 5.2 – Fit Quality versus ρ for 80% State of Charge

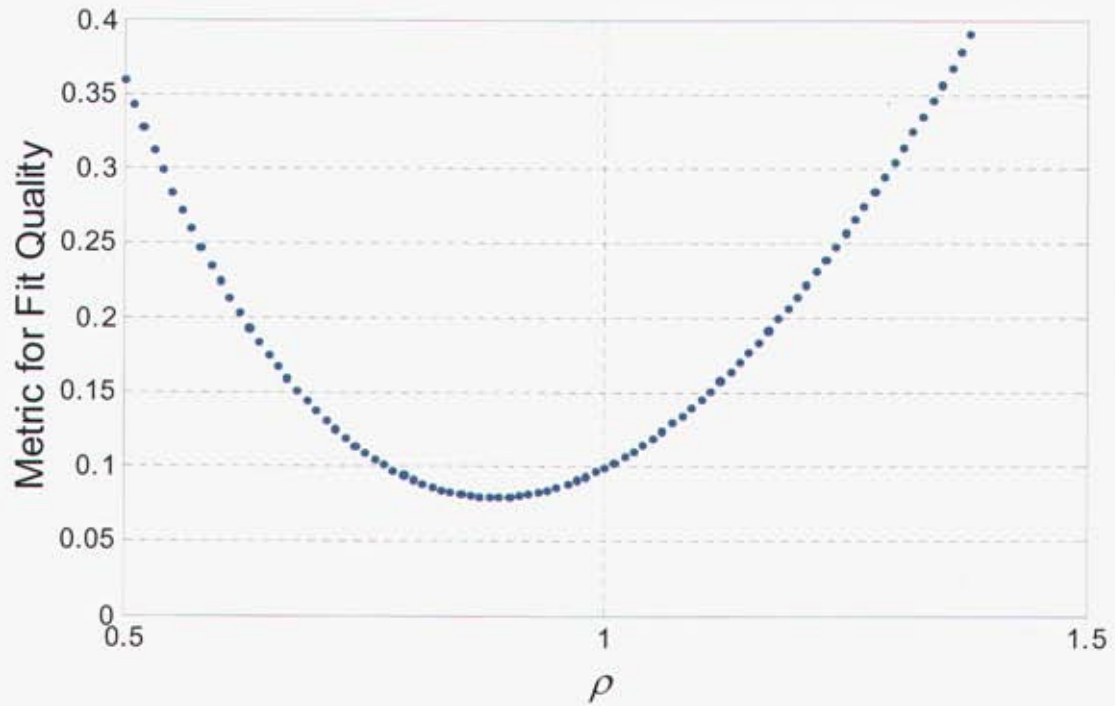


Figure 5.3 – Fit Quality versus ρ for 100% State of Charge

Table 5.2 Estimates of Model Parameters (with standard errors)

	$\hat{\beta}_0$ ($\hat{\sigma}_{\hat{\beta}_0}$)	$\hat{\beta}_1$ ($\hat{\sigma}_{\hat{\beta}_1}$)	Estimated Activation Energy: $\hat{E}_a = -R \cdot \hat{\beta}_1$
60% SOC	10.85 (.21)	-4.83×10^3 (1.5×10^2)	9.7 kcal per mole
80% SOC	15.72 (.56)	-6.26×10^3 (1.8×10^2)	12.5 kcal per mole
100% SOC	12.13 (.40)	-4.99×10^3 (1.3×10^2)	10.0 kcal per mole

Figures 5.4, 5.5, and 5.6 illustrate how the data in terms of $Y_i = \log\left\{\frac{-\log(Z(X_i))}{t_i}\right\}$, relate to the fitted model $\hat{Y}_i = \hat{\beta}_0 + \hat{\beta}_1 \cdot X_i$, where $X_i = T_i^{-1}$ for each state of charge. A solid straight line denotes the fitted model. An asterisk denotes each experimental observation. In general, the models represent the experimental data reasonable well. An exception is the apparent inconsistent performance of the cells stored at 45 degrees C storage in the case of 80% SOC.

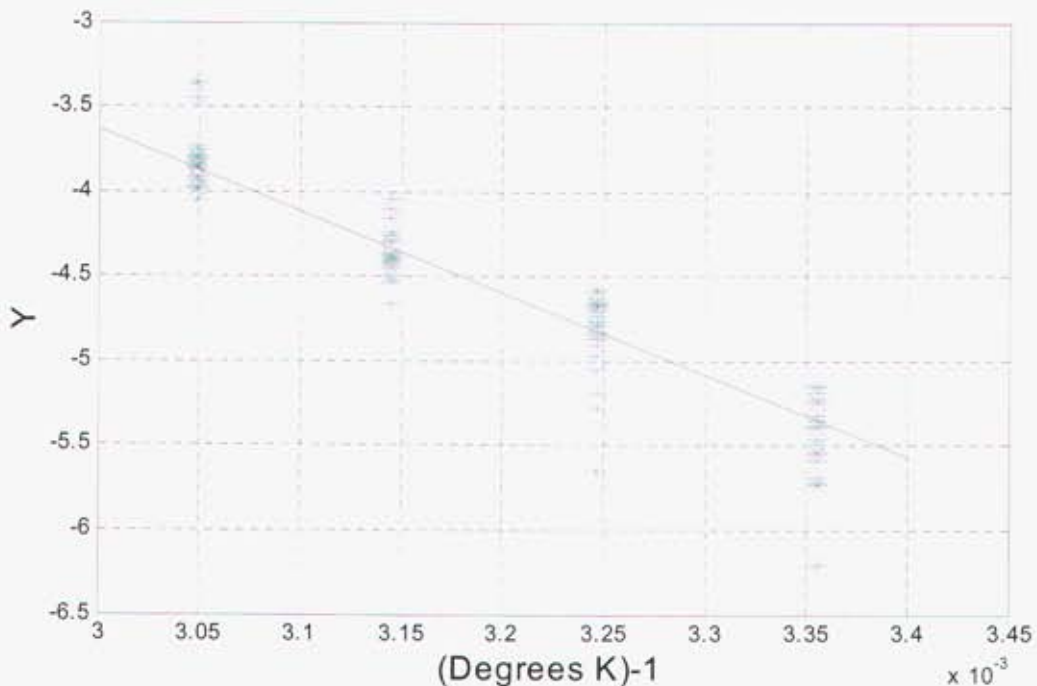


Figure 5.4 – Composite Arrhenius Plot for 60% State of Charge

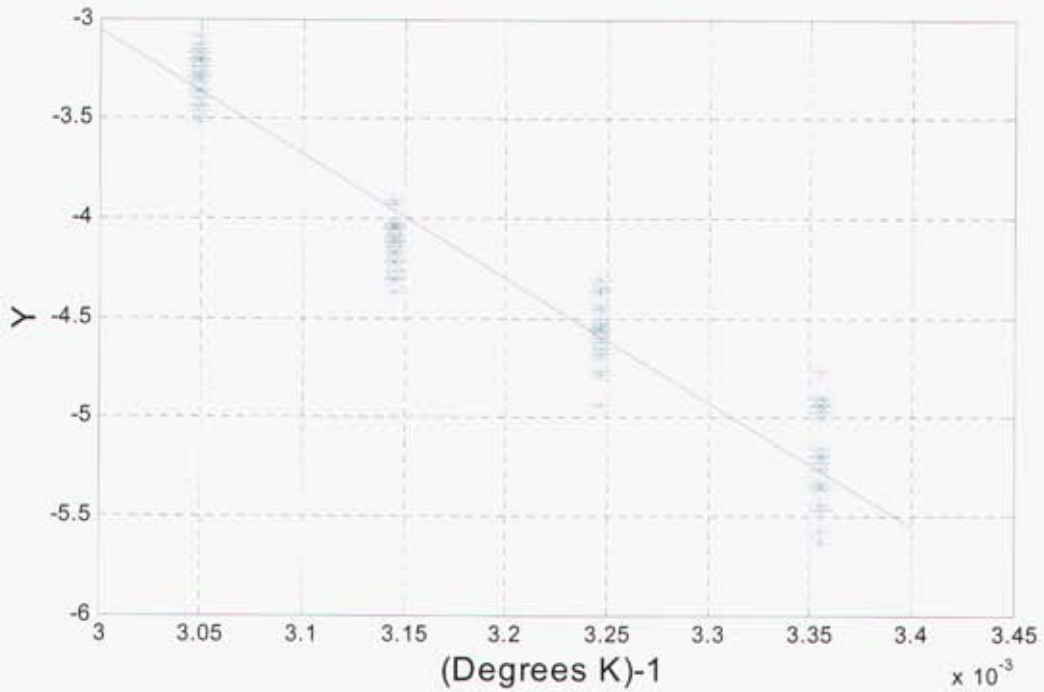


Figure 5.5 – Composite Arrhenius Plot for 80% State of Charge

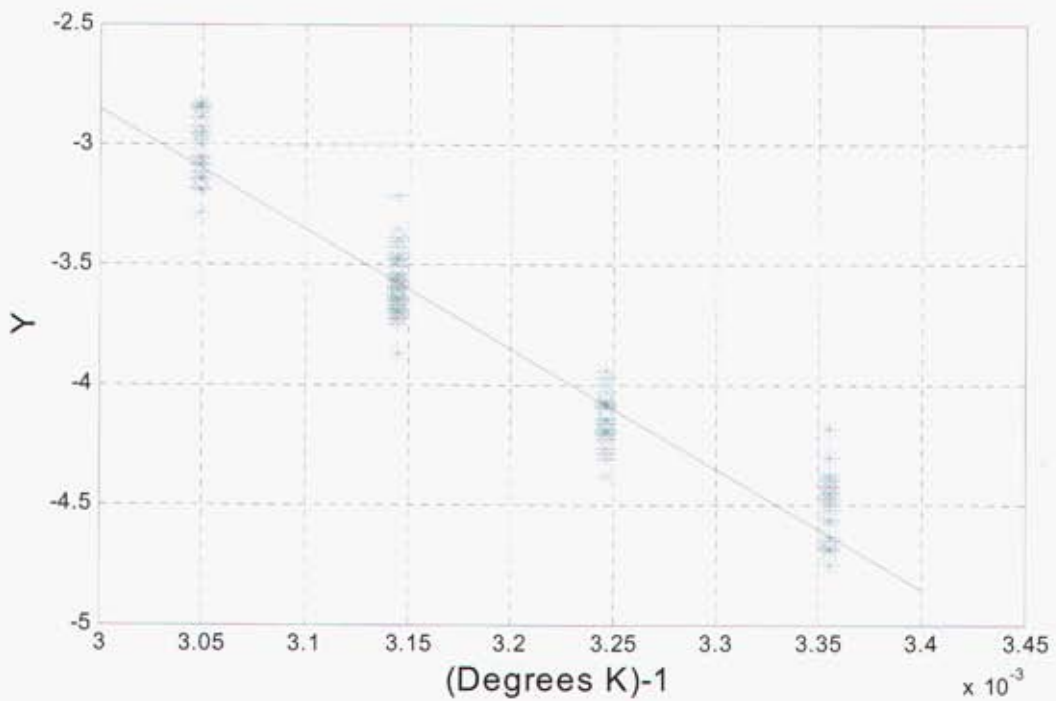


Figure 5.6 – Composite Arrhenius Plot for 100% State of Charge

Figures 5.7, 5.8, and 5.9 illustrate how well the observed relative power (Z_i) relates to the fitted model that gives predicted relative power ($\hat{Z}_i = \exp\left\{-\exp\left(\hat{\beta}_0 + \hat{\beta}_1 \cdot \frac{1}{T_i}\right) \cdot t_i\right\}$) for each state of charge. Different symbols are used to denote the storage temperature associated with each observation. The solid *line of identity* is used to facilitate the comparison of observed and predicted relative power.

Some deviations from the models are apparent. For example, in Figure 5.7 (60% SOC), the predicted relative power for each storage temperature seems to exhibit a parabolic pattern about the line of identity. That is, predictions associated with early time (e.g., week 4) and late time (e.g., week 32) generally exceed the actual power that is observed. On the other hand, the predictions associated with mid time (e.g., 20 weeks) are generally less than the measured relative power. This effect is consistent for cells stored at each of the four storage temperatures (particularly in the case of the 55 degree C data). Despite this effect, the model relates reasonable well to the experimental data and is useful for obtaining a good estimate of mean cell life.

Also, in Figure 5.8 (80% SOC), it is clear that the 45 degree C data are inconsistent with the model and the data associated with the other storage temperatures. Perhaps the poor fit illustrated in Figure 5.8 relates to the inconsistent estimate of activation energy in the 80% SOC case.

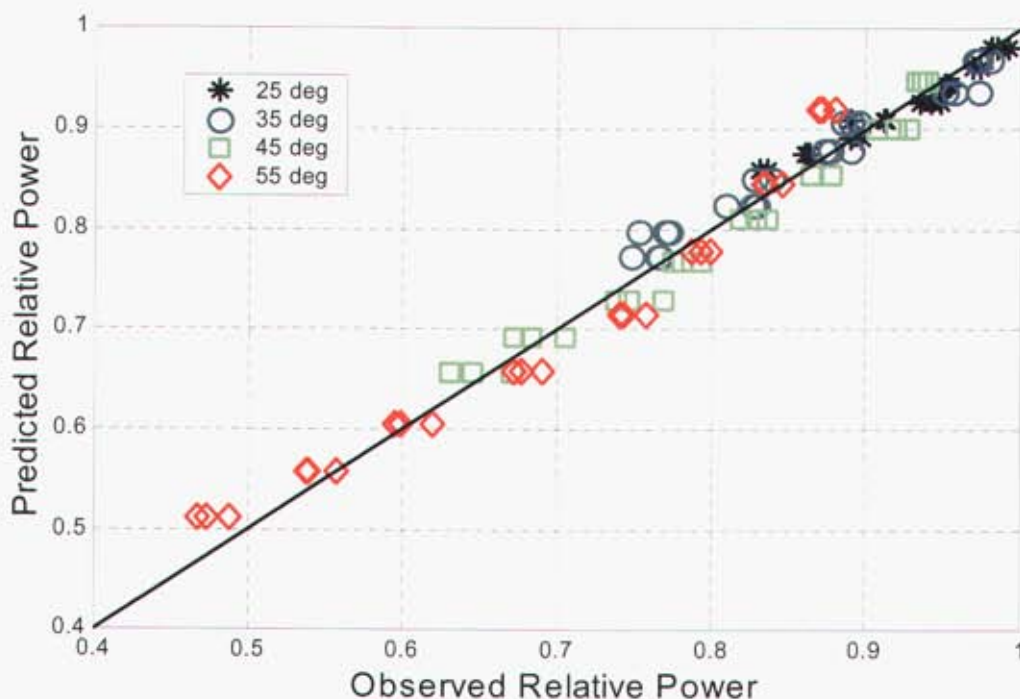


Figure 5.7 – Predicted versus Observed Relative Power for 60% State of Charge

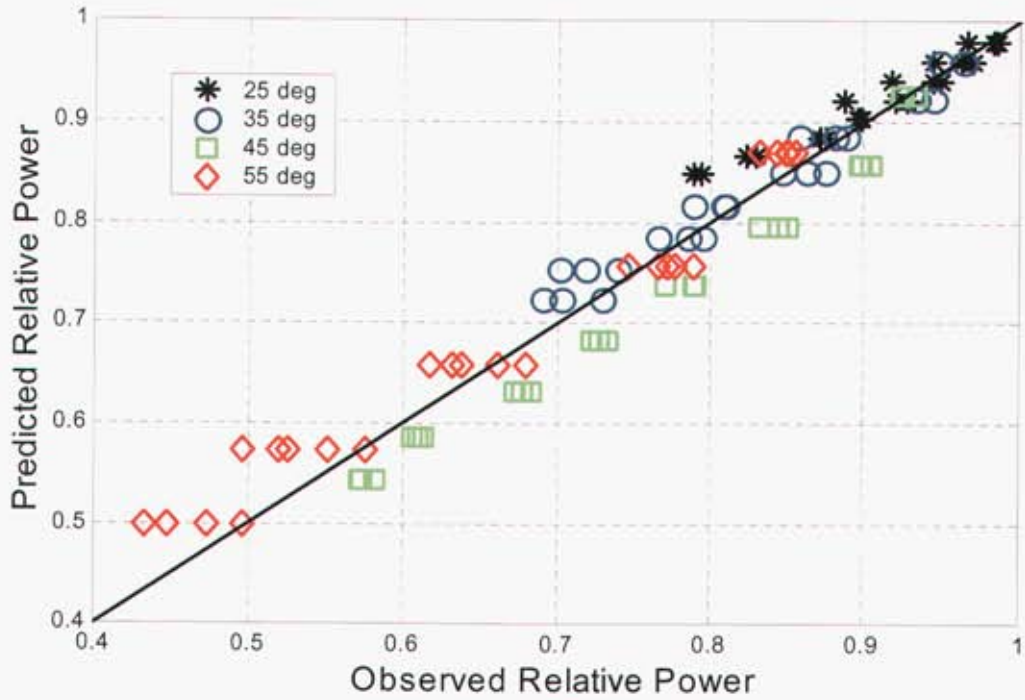


Figure 5.8 – Predicted versus Observed Relative Power for 80% State of Charge

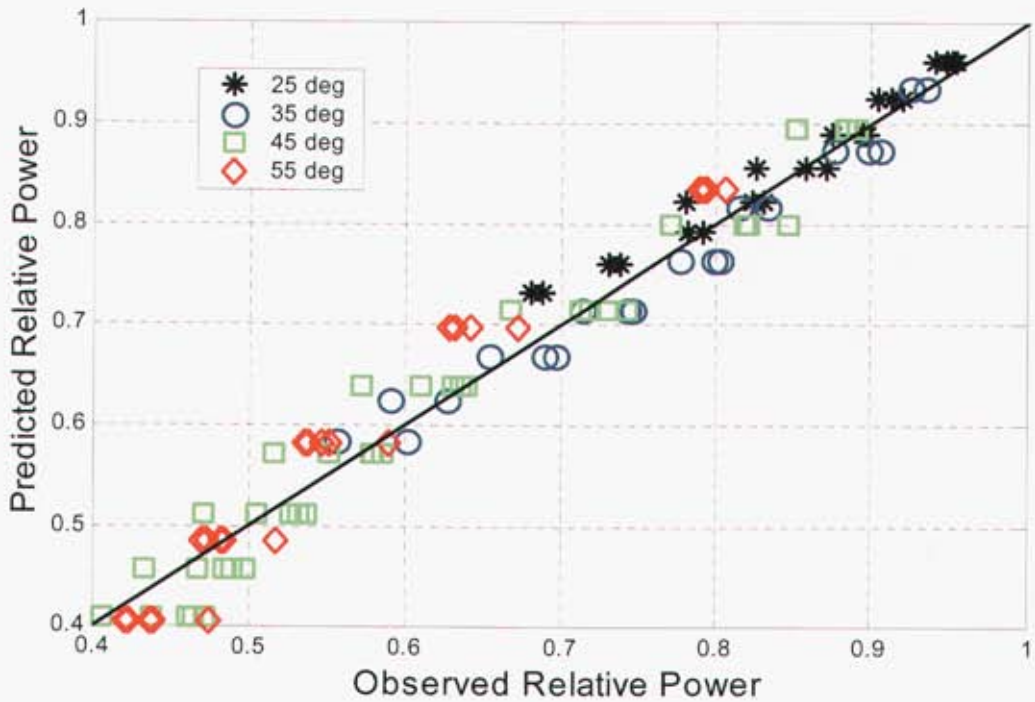


Figure 5.9 – Predicted versus Observed Relative Power for 100% State of Charge

5.2.1 Estimate of Mean Cell Lifetime

Here the method for estimating the mean cell lifetime (described in Section 4.3) is applied to the GEN-2 accelerated degradation data. The threshold performance is defined to be $Z_{thresh} = .77$. The target storage temperature and SOC are 25°C and 60%, respectively. Thus, we use the model specific for SOC=60% with $\mathbf{x} = [1 \ (273 + 25)^{-1}]$ and $\rho = 1$. The estimated mean cell

$$\text{lifetime is } \hat{t}_{life} = \exp\left\{\frac{\log(-\log(Z_{thresh})) - \mathbf{x}\hat{\boldsymbol{\beta}}_{final}}{\rho}\right\} = \frac{-\log(Z_{thresh})}{\exp(\mathbf{x}\hat{\boldsymbol{\beta}}_{final})} = 55.1 \text{ weeks.}$$

$Var(\hat{t}_{life}) = \hat{t}_{life}^2 \cdot \mathbf{x}^T \cdot Cov(\hat{\boldsymbol{\beta}}_{final}) \cdot \mathbf{x} = 3.7$, so that an approximate 95% confidence interval for the mean cell lifetime is $\hat{t}_{life} \pm 2 \cdot \sqrt{Var(\hat{t}_{life})} = 55.1 \pm 3.7$ weeks. On a related note, Figure 5.10 presents the estimated average power fade versus time with associated 95% confidence limits.

It is interesting to construct a model with $\rho = 1.08$. Then an approximate 95% confidence interval for the mean cell lifetime is $\hat{t}_{life} \pm 2 \cdot \sqrt{Var(\hat{t}_{life})} = 51.1 \pm 3.4$ weeks. Based on Figure 5.1 there is very little to distinguish these two cases of ρ in terms of quality of fit. This unaccounted for uncertainty in ρ means that the uncertainty limits are narrower than they should be.

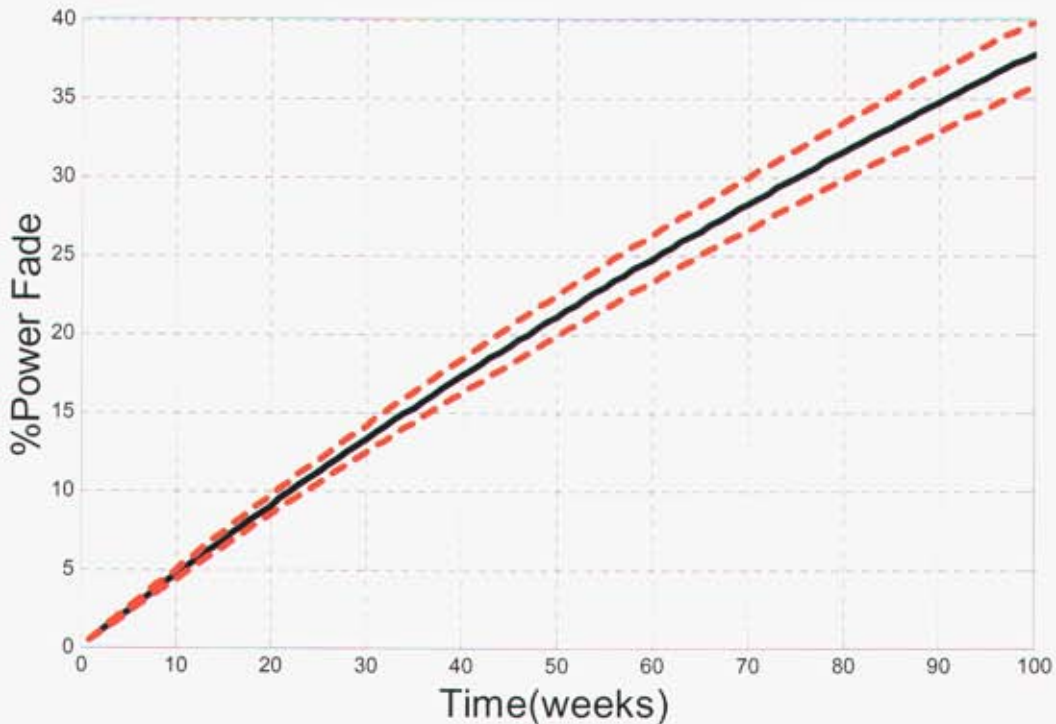


Figure 5.10 – Estimated Power Fade versus Time (with 95% confidence limits), 60% State of Charge, 25°C ($\rho=1.00$)

5.2.2 Augmenting With Additional Cells

In the case of this experiment, the uncertainty in cell lifetime is sufficiently small such that no additional cells were needed. Note that one could use the methodology described in Section 3.4 to evaluate the potential benefit in testing additional cells to reduce the uncertainty of the average cell lifetime.

5.3 Second Data Analysis - Following 44 weeks of Aging

The various predictive models that were developed were applied to the additional power fade data. Figure 5.11 displays the 25^o C / 60% SOC model (red solid line) overlaid with the observed power fade measurements through 44 weeks of aging (blue asterisks). Power fade measurements taken after 32 weeks did not influence the model building. It is clear that these later measurements are not predicted particularly well by the model. This provides the motivation for additional modeling efforts regarding the SNL data. However, it is important to note that the power fade model displayed in Figure 5.11 proved to be reasonably accurate (through 52 weeks of aging) in the case of Gen2 cells aged at 25^o C and 60% SOC at INEEL. Evidently the reference performance tests conducted at SNL were somewhat more degrading than the tests conducted at INEEL.

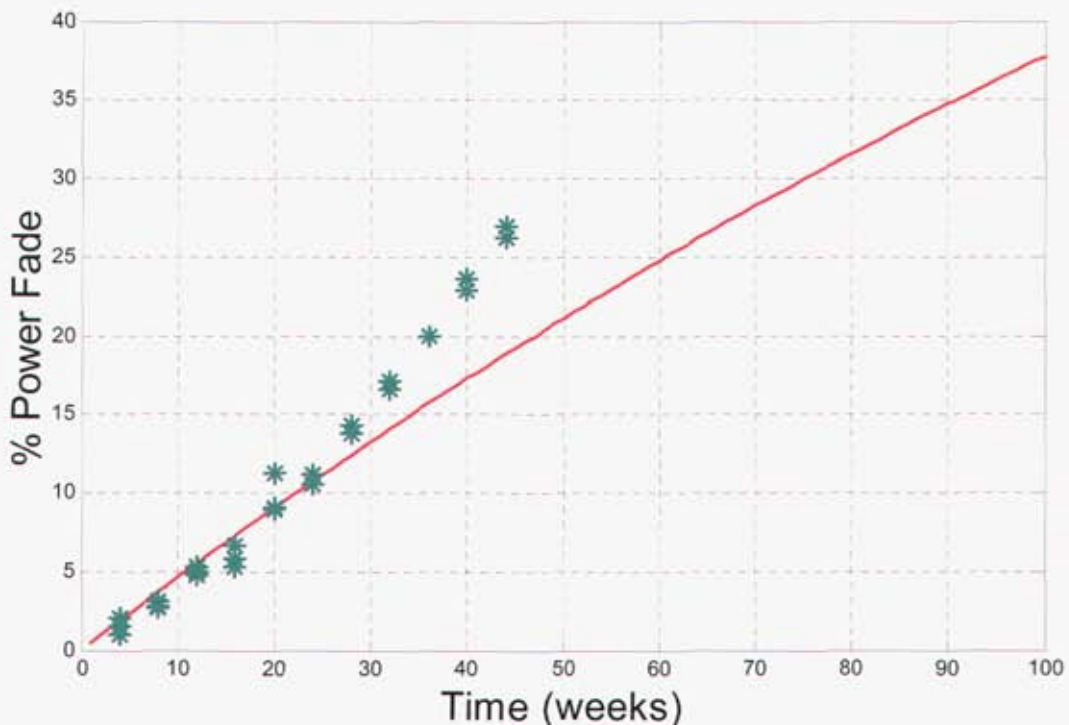


Figure 5.11 – Estimated Power Fade and Observed Power Fade versus Time, 60% State of Charge, 25^o C ($\rho=1.00$)

With the additional data through 44 weeks it is clear that the model defects discussed in Section 4.2 are important. Therefore, the second modeling effort is concerned with those defects. The overriding philosophy of this modeling effort is to seek a single model that operates over a wide (and clearly understood) range of temperature and SOCs. Desired characteristics of the model include simplicity (few model parameters) and high fidelity in regions where high fidelity is required. High fidelity much beyond the point of degradation that defines cell lifetime (23% power fade) is not a high priority.

The model building process included the following steps. First, the time dependence of power fade was investigated. In particular, graphical analyses were performed in order to determine a transformation of time (via a time exponent) that *linearizes* the relationship of power fade with transformed time. The *slope* and *intercept* of the linear relationship were estimated for each aging condition as determined by temperature and SOC. Next, the estimated intercept and slope were modeled as a function of temperature and SOC. Regions in the temperature / SOC plane where the estimated slope and intercept are consistent with simple models were identified. Finally, a global model of power fade (as a function of temperature and SOC) was developed based on forms of the *slope* and *intercept* models and the experimental data within the consistent regions in the temperature / SOC plane.

5.3.1 Time Dependence of Power Fade

Figure 5.12 illustrates the relationship between relative power and time in the case of 60% SOC for the various aging temperatures. Graphical analysis, investigating various fractional powers of time as potential transformations, was used to determine a transformation of time (t^ρ) that *linearizes* the relationship of power fade with transformed time for all aging conditions. This analysis led to the selection of $\rho = 3/2$ as a useful transformation. Figures 5.13, 5.14, and 5.15 illustrate the utility of $t^{3/2}$ as a linearizing transformation over all states of charge and temperatures. Although this relationship breaks down when the power fade exceeds 40%, good model fidelity is maintained well beyond the point of degradation that defines cell lifetime. For purposes of visual reference, solid lines are overlaid on the data to indicate the quality of the linearizing transformation.

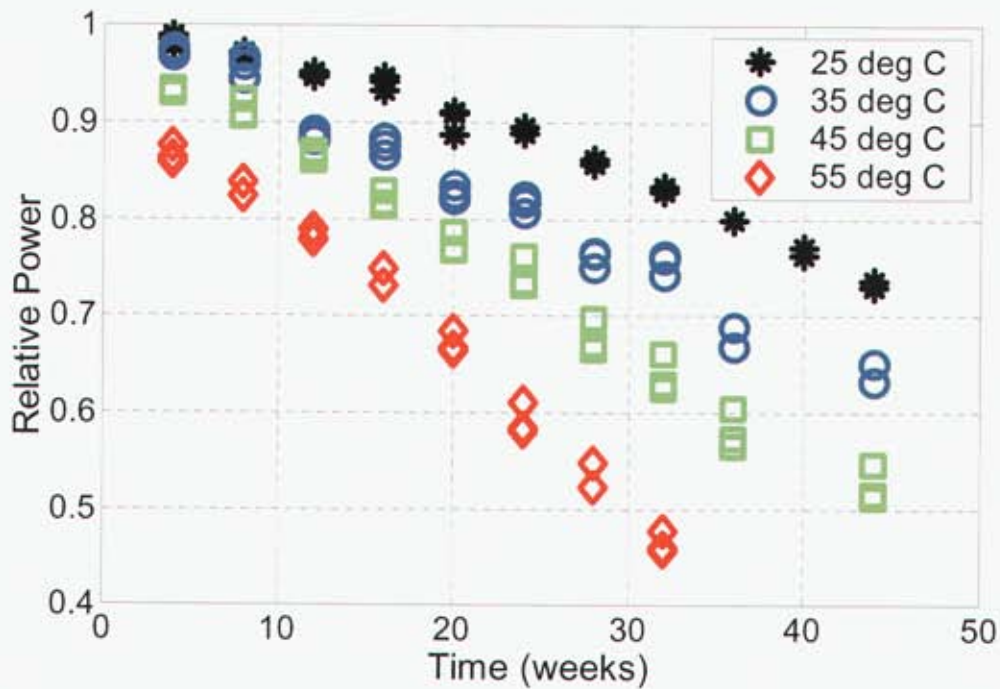


Figure 5.12 – Relative Power versus Time (60% State of Charge)

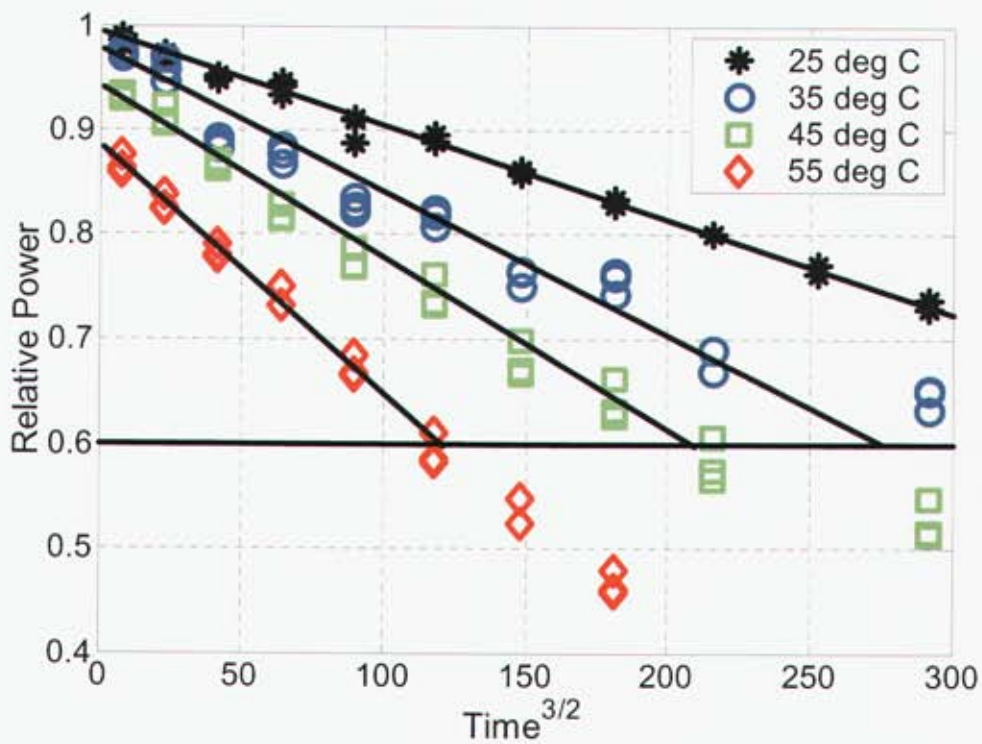


Figure 5.13 – Relative Power versus Time^{3/2} (60% State of Charge)

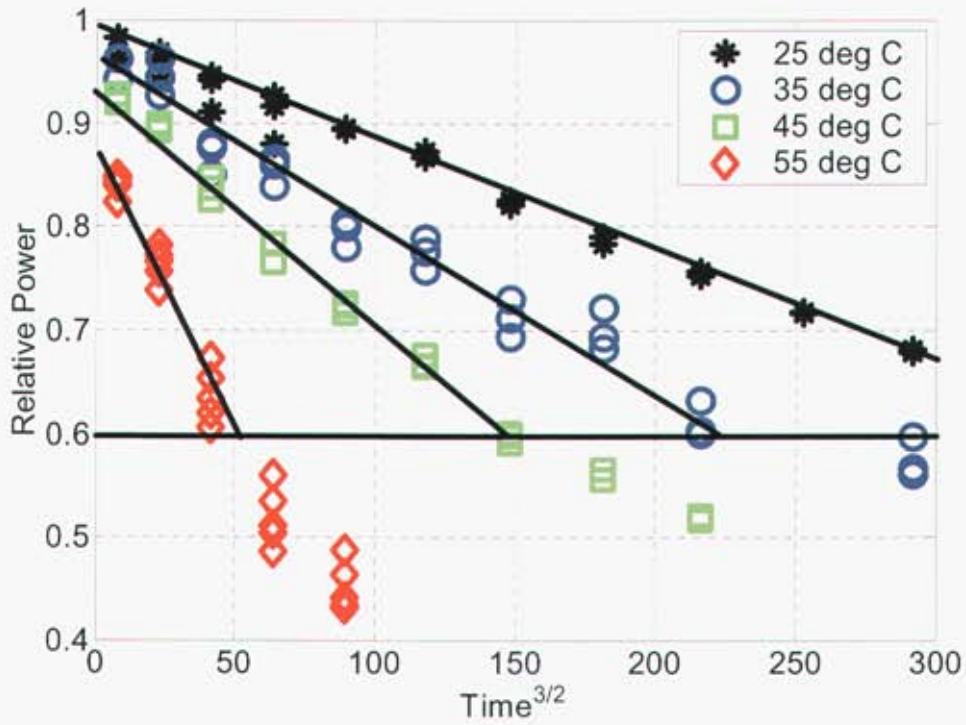


Figure 5.14 – Relative Power versus Time^{3/2} (80% State of Charge)

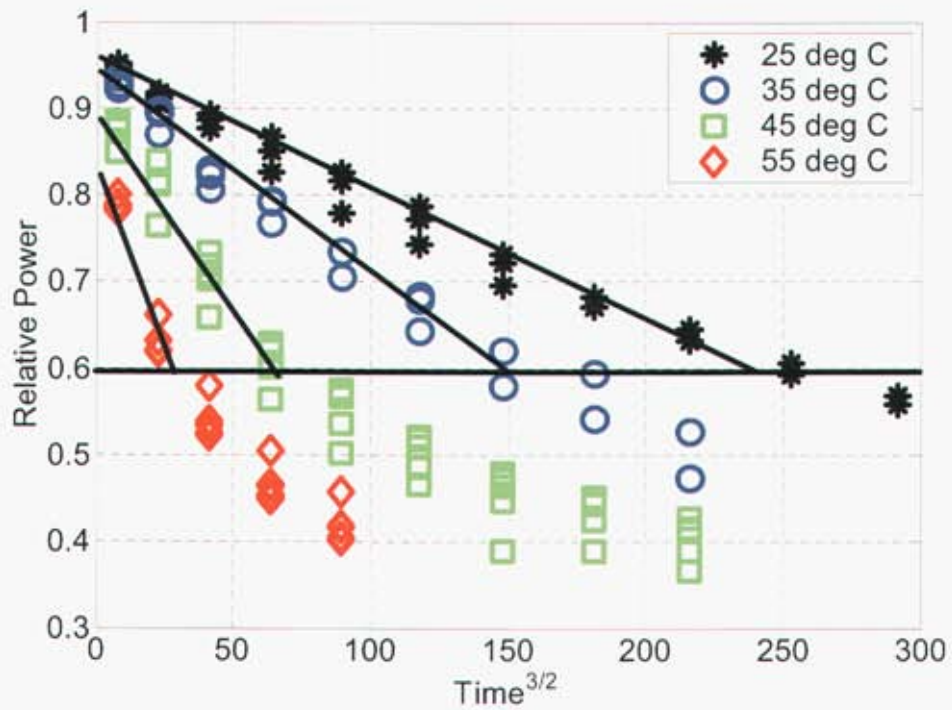


Figure 5.15 – Relative Power versus Time^{3/2} (100% State of Charge)

5.3.2 Generalized Model of Power Fade

Motivated by the observed time dependence, a general model form for power fade is $Z(t;T,SOC) = A(T,SOC) - B(T,SOC) \cdot t^{3/2}$, where $Z(t;T,SOC)$ is the relative power of a cell (compared to its initial state) after aging the cell at temperature (T) and state of charge (SOC) for time $t \geq 4$ weeks. Appropriate forms for $A(T,SOC)$ and $B(T,SOC)$ were determined by the analysis that follows. By definition, $Z(0;T,SOC) = 1$. The difference between $Z(0;T,SOC)$ and $A(T,SOC)$, represents the cumulative effect of a relatively rapid degradation process that depends on T and SOC . Apparently, this rapid degradation is nearly complete within 4 weeks. Concurrently, there is a second degradation process that is operating at a much slower rate. The relative power lost in this second process is represented by $-B(T,SOC) \cdot t^{3/2}$.

In order to make this model form useful, we need to develop models that reflect how the intercept (A) and the slope (B) vary over the aging conditions given by temperature and SOC. For each aging condition (and limited to cases where the observed power fade is less than 40%), a robust regression procedure was used to estimate the slope and intercept of the observed time dependence. The robust regression procedure is based on minimizing the sum of the absolute value of deviations about the fitted line rather than minimizing the sum of the squared deviations about the fitted line (least squares). Thus it is relatively unaffected by discordant experimental data. Figures 5.16 and 5.17 illustrate transformations of the estimated values of the intercept and slope versus the various aging conditions.

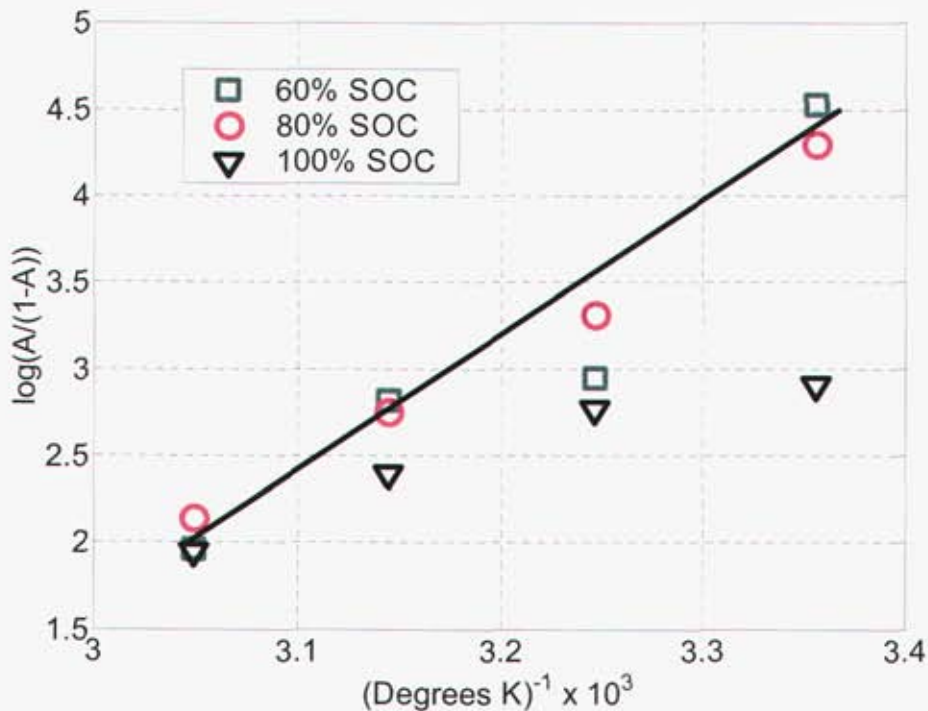


Figure 5.16 – Logit(A) versus $1/\text{Temperature}$ and SOC

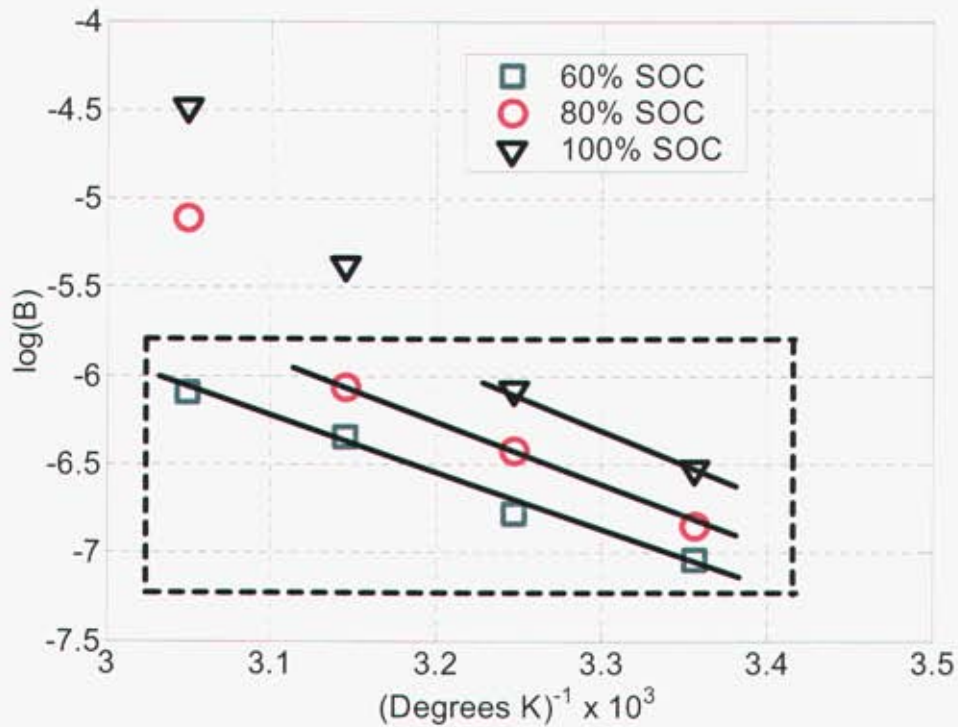


Figure 5.17 – Log (*B*) versus 1/Temperature and SOC

As seen in Figure 5.16, the logit transformation provides a useful means to represent the relationship between the estimated intercept (*A*) and the various aging conditions. The logit of *A*

is $\log\left(\frac{A}{1-A}\right)$. A useful property of the logit transformation (that facilitates the modeling

process) is that it maps an input (like relative power) that varies in the interval (0,1) to the real line $(-\infty, \infty)$. In general, the estimated intercepts associated with the 60% SOC and 80% SOC data relate well to the model that is represented by the solid line in Figure 5.16. That is,

$\log\left(\frac{A}{1-A}\right) = a_0 + a_1 \cdot \frac{1}{T}$. The clear exception is the 35^o C data (which exhibit some behavior

that is not understood – see the staircase degradation in Figures 5.13, 5.14, and 5.15).

Nevertheless, it is considered that all of the 60% and 80% data are consistent in the modeling

sense. Note that the inverted logit transform is $A = \frac{\exp\left(a_0 + a_1 \cdot \frac{1}{T}\right)}{1 + \exp\left(a_0 + a_1 \cdot \frac{1}{T}\right)}$.

In terms of the estimated slope (B), a *useful* model is given by $\log(B) = b_0 + b_1 \cdot \frac{1}{T} + b_2 \cdot SOC$, or

$B = \exp\left(b_0 + b_1 \cdot \frac{1}{T} + b_2 \cdot SOC\right)$. Figure 5.17 illustrates the utility of this model for the portion of the temperature / SOC plane that is within the dashed rectangle. The parallel lines (one per SOC) added for visual perspective and superimposed on the B s indicate that the effect of temperature on the B s is consistent across SOC s. The fact that the parallel lines are roughly equidistant supports the linear dependence on SOC that is provided through b_2 .

Substituting the expressions for A and B into $Z(t; T, SOC) = A(T, SOC) - B(T, SOC) \cdot t^{3/2}$ yields

$$Z(t; T, SOC) = \frac{\exp\left(a_0 + a_1 \cdot \frac{1}{T}\right)}{1 + \exp\left(a_0 + a_1 \cdot \frac{1}{T}\right)} - \exp\left(b_0 + b_1 \cdot \frac{1}{T} + b_2 \cdot SOC\right) \cdot t^{3/2}.$$

This global model, involving five parameters (a_0 , a_1 , b_0 , b_1 , and b_2), is valid within the region defined by 60% SOC (25°C to 55°C), 80% SOC (25°C to 45°C), and 100% SOC (25°C to 35°C) and for $t \geq 4$ weeks. . The model parameters were estimated by robust nonlinear regression using data within the aging conditions identified and further restricted such that observations with power fade exceeding 40% were omitted. Estimates of the model parameters are: $\hat{a}_0 = -21.01$, $\hat{a}_1 = 7.585 \times 10^3$, $\hat{b}_0 = 4.0387$, $\hat{b}_1 = -3.547 \times 10^3$, and $\hat{b}_2 = .01331$.

Figures 5.18 and 5.19 illustrate the degree to which the model (solid line) represents the observed % power fade (symbols). Note that %Power Fade = $100 \cdot (1 - Z)$.

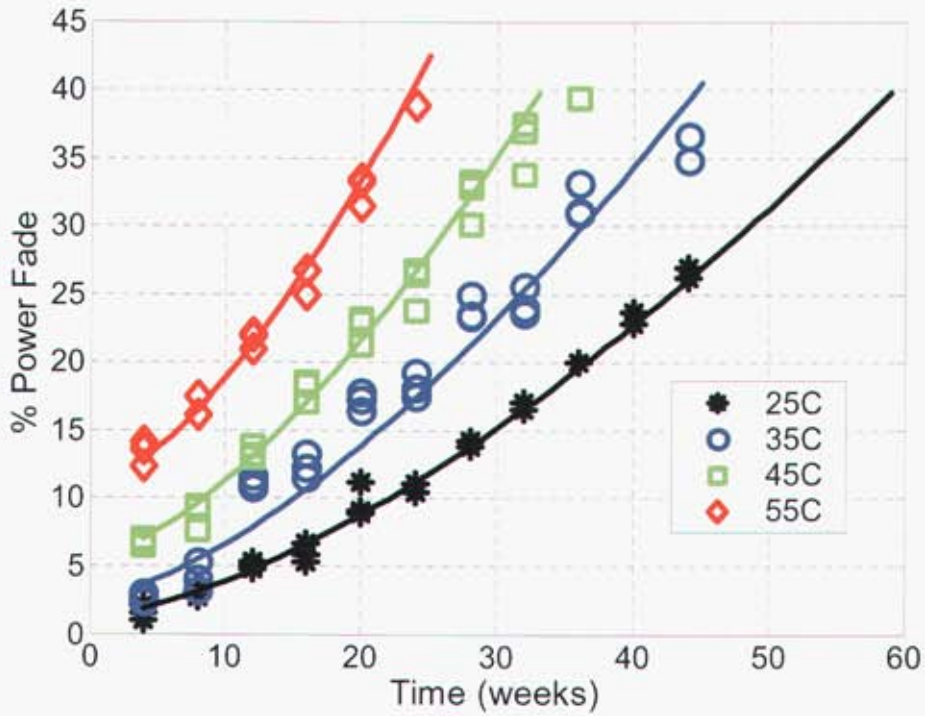


Figure 5.18 – % Power Fade versus Time: 60% SOC

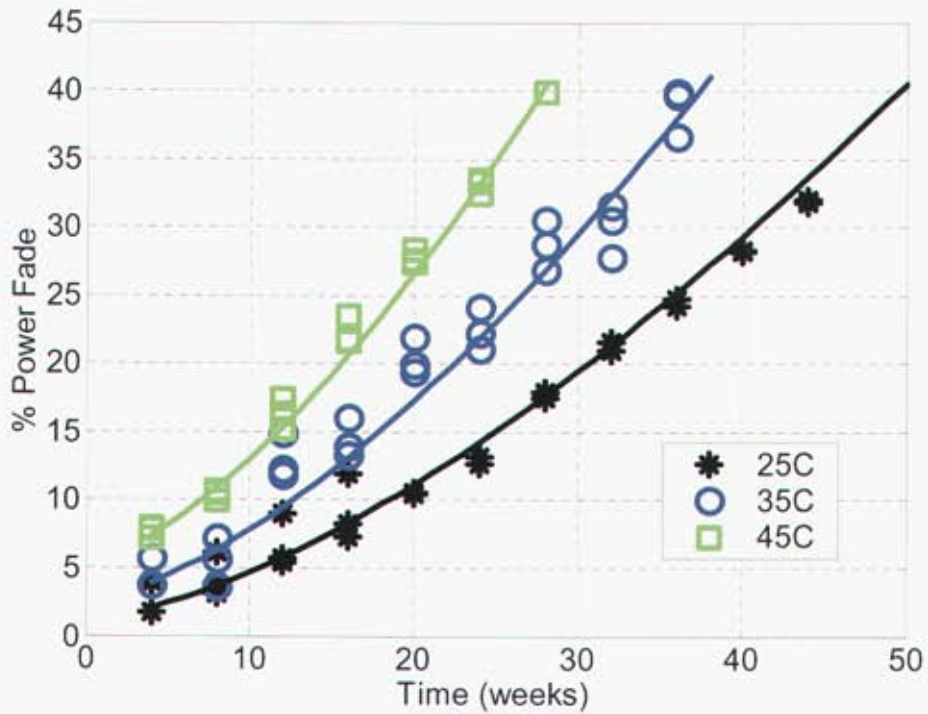


Figure 5.19 – % Power Fade versus Time: 80% SOC

Statistical analysis of the additional power fade data has led to the development of a general power fade model (involving dual concurrent degradation mechanisms) that is applicable over a range of aging conditions. Degradation associated with the first mechanism is relatively rapid and appears to be substantially complete within four weeks. For SOC between 60% and 80%, the degradation is very consistent and appears to be driven solely by temperature. At 100% SOC, the degradation is more severe and has a different temperature dependence. The second mechanism exhibits degradation that is proportional to $time^{3/2}$. [Note that it was also observed that the area specific impedance (for a fixed aging condition), on which the power calculation is based, is also proportional to $time^{3/2}$.] This mechanism appears to be consistent within the region defined by 60% SOC (25°C to 55°C), 80% SOC (25°C to 45°C), and 100% SOC (25°C to 35°C), i.e., over 75% of the test conditions. The global model that was developed provides a very accurate representation of the observed power fade data to the point where 60% of the original power remains for all 60% SOC and 80% SOC aging conditions except for 55°C at 80% SOC. Beyond 60% power fade, the model does not predict well. This could be due to consumption of reactants. In any event, there is little current interest in understanding power fade beyond 60%. A similar approach could be applied to capacity fade or any other metric of cell performance.

As illustrated in Figures 5.18 and 5.19, the model applies to degradation beyond 4 weeks of aging. The time dependence of this early degradation is unknown based on the absence of RPTs between 0 and 4 weeks. The following experiment could provide some significant insight regarding the nature of the rapid temperature-dependent degradation of Gen2 cells that was observed.

Choose a single SOC (60% or 80%), three aging temperatures (say 25C, 40C, and 55C), and 3 cells per temperature. After measuring the power of the nine fresh cells, subject them to isothermal aging and re-measure the power after {0, .5, 1, 2, 4} weeks of aging. Analysis of the aging data would provide the time dependence of power fade during the first 4 weeks of aging.

6. Summary and Future Work

This document discusses experimental design and data analysis protocols for accelerated degradation experiments in the context of Li-ion cells. These protocols should provide the necessary tools for a scientist to estimate (at a practical level) the average cell life that might be expected from a new design so long as cell degradation approximately follows first-order rate kinetics with a single mechanism in a single aging environment. While the experimental protocols are generally applicable, the data analysis protocols do not necessarily relate to other degradation kinetics.

Motivated by inadequacies of the simple first-order rate model when applied to data through 44 weeks, an improved model with two concurrent degradation mechanisms was developed. While the general applicability of this model has not been determined, the method by which it was developed should have general use for predicting life of rechargeable batteries of various chemistries.

We plan to expand this work to include protocols for other kinetics models. It would be useful to explore the other effects that multiple mechanisms might have on the observed degradation data. It then would be useful to develop experimental protocols and other diagnostic procedures that would allow an analyst to detect the presence of multiple mechanisms. Finally, it would be useful to further develop protocols (experimental design and modeling) that facilitate modeling multiple mechanisms.

The current experimental design and data analysis protocols can provide lifetime assessments that relate to the degradation of cells that age in static environments. In its actual use, a cell will experience a wide range of environments. In addition, assumptions that the performance degradation of a cell beyond its current performance state depends only on its current state and not how it reached that state may be overly simplistic and grossly incorrect. Thus, it is of interest to characterize cell degradation over dynamic aging conditions. Currently, methods for selecting the dynamic aging environments to be used for developing and/or validating degradation models are unavailable and thus could be the subject for valuable research. Furthermore, if degradation in dynamic aging environments is found to be complex, additional effort will be required to develop useful degradation models.

7. References

- Box G. E. P. and Draper N. E., *Empirical Model-Building and Response Surfaces*, 1997, Wiley.
- Box, G. E. P., Hunter W. G., and Hunter J. S., *Statistics for Experimenters*, 1978, Wiley.
- Boulanger M. and Escobar L. A., Experimental Design for a Class of Accelerated Degradation Tests, *Technometrics*, 1994, 260-272.
- Case, H. L. *SNL Test Plan for Advanced Technology Development GEN 2 Lithium-ion Cells*, 2002
- Castellan G. W., *Physical Chemistry (2nd Edition)*, 1971, Addison-Wesley.
- Chan V. and Meeker W. Q., Estimation of Degradation-Based Reliability in Outdoor Environments, Technical Report (Statistics Department), 2001, Iowa State University.
- Draper, N. R. and Smith, H., *Applied Regression Analysis (2nd Edition)*, 1981, Wiley.
- Efron B. and Tibshirani R. J., *An Introduction to the Bootstrap*, 1993, Chapman and Hall.
- Escobar L. A. and Meeker W. Q., Planning Accelerated Life Tests With Two or More Experimental Factors, *Technometrics*, 1995, 411-427.
- Meeker W. Q., Escobar L. A., and Lu C. J., Accelerated Degradation Tests: Modeling and Analysis, *Technometrics*, 1998, 89-99.
- Meeker W. Q. and Escobar L. A., Chapter 21 – Accelerated Degradation Tests, *Statistical Methods for Reliability Data*, 1998, Wiley.

Ripley, B.D., *Spatial Statistics*, 1981, Wiley.

Speitel, K. F., Chapter 8.2 – Measurement Assurance, *Handbook of Industrial Engineering*, 1982, Wiley.

Weigand, D. E. and Thomas E. V., Capacity Loss Predictions for Active Primary Cells Using Accelerated Aging, 2002, presented at the 202nd Meeting of the Electrochemistry Society in Salt Lake City, UT – October 22, 2002.

8. APPENDIX A — Fractional Factorial Designs

Table 8.1 – 3 Factor Design

Treatment Combination	Factor#1	Factor#2	Factor#3
1	-	-	+
2	-	+	-
3	+	-	-
4	+	+	+

Table 8.2 – 4 Factor Design

Treatment Combination	Factor#1	Factor#2	Factor#3	Factor#4
1	-	-	-	-
2	-	-	+	+
3	-	+	-	+
4	-	+	+	-
5	+	-	-	+
6	+	-	+	-
7	+	+	-	-
8	+	+	+	+

Table 8.3 – 5 Factor Design

Treatment Combination	Factor#1	Factor#2	Factor#3	Factor#4	Factor#5
1	-	-	-	+	+
2	-	-	+	+	-
3	-	+	-	-	+
4	-	+	+	-	-
5	+	-	-	-	-
6	+	-	+	-	+
7	+	+	-	+	-
8	+	+	+	+	+

Table 8.4 – 6 Factor Design

Treatment Combination	Factor#1	Factor#2	Factor#3	Factor#4	Factor#5	Factor#6
1	-	-	-	+	+	+
2	-	-	+	+	-	-
3	-	+	-	-	+	-
4	-	+	+	-	-	+
5	+	-	-	-	-	+
6	+	-	+	-	+	-
7	+	+	-	+	-	-
8	+	+	+	+	+	+

Table 8.5 – 7 Factor Design

Treatment Combination	Factor#1	Factor#2	Factor#3	Factor#4	Factor#5	Factor#6	Factor#7
1	-	-	-	+	+	+	-
2	-	-	+	+	-	-	+
3	-	+	-	-	+	-	+
4	-	+	+	-	-	+	-
5	+	-	-	-	-	+	+
6	+	-	+	-	+	-	-
7	+	+	-	+	-	-	-
8	+	+	+	+	+	+	+

9. APPENDIX B – Plackett-Burman Design

Table 9.1 – Plackett-Burman Design

Treatment Combination	F1	F2	F3	F4	F5	F6	F7	F8	F9	F10	F11
1	+	+	+	+	+	+	+	+	+	+	+
2	-	-	+	-	-	-	+	+	+	-	+
3	+	-	-	+	-	-	-	+	+	+	-
4	-	+	-	-	+	-	-	-	+	+	+
5	+	-	+	-	-	+	-	-	-	+	+
6	+	+	-	+	-	-	+	-	-	-	+
7	+	+	+	-	+	-	-	+	-	-	-
8	-	+	+	+	-	+	-	-	+	-	-
9	-	-	+	+	+	-	+	-	-	+	-
10	-	-	-	+	+	+	-	+	-	-	+
11	+	-	-	-	+	+	+	-	+	-	-
12	-	+	-	-	-	+	+	+	-	+	-

EXTERNAL DISTRIBUTION:

- 1 Daniel P. Abraham
Chemical Engineering Division
Argonne National Laboratory
Electrochemical Technology & Basic Sciences
9700 South Cass Avenue, Bldg. 205
Argonne, IL 60439
- 1 Mohamed Alamgir
Compact Power, Inc.
1200 South Synthes Avenue
Monument, CO 80132
- 1 Khalil Amine
Chemical Engineering Division
Argonne National Laboratory
Electrochemical Technology Program
9700 Cass Avenue
Argonne, IL 60439
- 1 Michele L. Anderson
Dept. of Engineering, Materials & Physical Sciences S&T
Office of Naval Research
800 North Quincy Street
Arlington, VA 22217
- 1 Cyrus N. Ashtiani
Department of Advanced Batteries and Fuel Cells
DaimlerChrysler Corporation
2730 Research Drive
Rochester Hills, MI 48309
- 1 Terrill B. Atwater
Department of Army Power
U.S. Army CERDEC
AMSEL-RD-C2-AP-B
Ft. Monmouth, NJ 07703
- 1 James A. Bames
Office of FreedomCAR and Vehicle Technologies
U.S. Department of Energy
Naval Surface Warfare Center
1000 Independence Avenue, SW
Washington, DC 20585

- 1 Vincent S. Battaglia
Chemical Engineering Division
Argonne National Laboratory
Building 205
9700 South Cass Avenue
Argonne, IL 60439
- 1 George E. Blomgren
Blomgren Consulting Services Ltd.
1554 Clarence Avenue
Lakewood, OH 44107
- 1 Ira D. Bloom
Chemical Engineering Division
Argonne National Laboratory
Building 205
9700 South Cass Avenue
Argonne, IL 60439
- 1 Ralph J. Brodd
Broddarp of Nevada, Inc.
2161 Fountain Springs Drive
Henderson, NV 89074
- 1 Ratnakumar V. Bugga
Electrochemical Technologies Group
Jet Propulsion Laboratory
4800 Oak Grove Drive
Pasadena, CA 91109
- 1 Dennis W. Dees
Chemical Engineering Division
Argonne National Laboratory
Building 205
9700 South Cass Avenue
Argonne, IL 60439
- 1 Joe DiCarlo
Lithion/Yardney
82 Mechanic Street
Pawcatuck, CT 06379

- 1 Tien Q. Duong
FreedomCAR & Vehicle Technologies Program
U.S. Department of Energy
1000 Independence Avenue, SW
Washington, DC 20585
- 1 Mohammad A. Habib
Materials & Processes Lab
General Motors R&D Center
MC 480-106-224
30500 Mound Road
Warren, MI 48090
- 1 Gary Henriksen
Chemical Engineering Division
Battery Technology Department
Argonne National Laboratory
Building 205
9700 South Cass Avenue
Argonne, IL 60439
- 1 T. Richard Jow
Army Research Laboratory
2800 Powder Mill Road
Adelphi, MD 20783
- 1 Peter B. Keller
Power Systems Branch
Naval Surface Warfare Center-Carderock
Code 644
9500 MacArthur Boulevard
West Bethesda, MD 20817-5700
- 1 Keith D. Kepler
Farasis Energy, Inc.
851 West Midway Avenue
Alameda, CA 94501
- 1 Tyler X. Mahy
Power Sources Center
CIA
2R4502 NHB
Washington, DC 20505

- 1 Vesselin G. Manev
Department of Lithium Battery Systems
Delphi Corporation
1601 Averill Avenue
Flint, MI 48556
- 1 Azzam N. Mansour
Code 644
Naval Surface Warfare Center-Carderock
9500 MacArthur Boulevard
West Bethesda, MD 20817-5700
- 1 James McBreen
Materials Science Department
Brookhaven National Laboratory
Building 555
Upton, NY 11973
- 1 Frank McLarnon
Lawrence Berkeley National Laboratory
Building 7OR0108 B
Berkeley, CA 94720
- 1 Theodore J. Miller
Department of Research and Advanced Engineering
Ford Motor Company
15050 Commerce Drive North
Dearborn, MI 48120
- 1 Robert W. Minck
Consultant - USABC
24161 Becard Drive
Laguna Niguel, CA 92677
- 1 Chester G. Motloch
Department of Transportation Technologies
INEEL
P.O. Box 1625
Idaho Falls, ID 83401
- 1 Ahmad Pesaran
Center for Transportation Technologies & Systems
National Renewable Energy Laboratory
1617 Cole Boulevard
Golden, CO 80401

- 1 William H. Schank
USABC Department
Ford Motor Company
15050 Commerre Drive North
Dearborn, MI 48120
- 1 Joseph F. Stockel
NRO/CIA
14675 Lee Road
Chantilly, VA 20151
- 1 Harshad Tataria
General Motors
MC 480 111 552
P.O. Box 901
30200 Mound Road
Warren, MI 48090-9010
- 1 William Tiedermann
Consultant
394 Douglas
Cedarburg, WI 53012
- 1 Hisashi Tsukamoto
Quallion L.L.C.
12744 San Fernando Road
Sylmar, CA 91342
- 1 Enoch I. Wang
Power Source Center
CIA
Washington, DC 20505
- 1 Irwin Weinstock
Sentech, Inc.
4733 Bethesda Avenue, Ste. 608
Bethesda, MD 20814
- 1 Randy B. Wright
INEEL
MS 3830
P.O. Box 1625
Idaho Falls, ID 83415-3830

1 Weibing Xing
Department of Research & Development
Wilson Greatbatch Technologies, Inc.
10,000 Wehrle Drive
Clarence, NY 14031

INTERNAL DISTRIBUTION:

3	MS	0613	D. L. Doughty, 2521
3		0613	E. P. Roth, 2521
1		0613	G. Nagasubramanian
1		0613	R. G. Jungst, 2525
10		0829	E. V. Thomas, 12323
1		0829	J. M. Sjulín, 12323
2		0899	Technical Library, 9616